Moldeing of microwave food processing and electromagnetic/thermal phenomena

Ben Q. Li, H. Yin and J. Tang
School of Mechanical & Materials Engineering
Department of Pure and Applied Mathematics
Department of Biosystems Engineering
Washington State University
Pullman, WA 99164

January 7, 2002

Overview of ongoing projects on numerical & physical modeling of electromagnetic/thermal phenomena

- Electromagnetic and electrostatic levitation of droplets in normal and micro gravity
- Magnetic field effects on g-jitter induced flows and mass transfer
- Integrated modeling of electrodynamic and transport (fluid flow, heat & mass transfer, thermal stresses) phenomena during optical single crystal growth
- Integrated modeling and optimization of microwave processing (jointly with Professors Tang and Yin)

Acknowledgement

- Funding agencies: NSF, NASA, DOE, DOD, Alcoa, Carbomedics Inc., III-V Incorporated, Dow Chemicals Company, Concurrent Technology, Inc. and Isothernal Spray Inc.

Objectives of this talk

- Discuss the FE, BE and FBE methods: their advantages and disadvantages
- Parallel computation: merits and drawbacks
- Modeling of coupled microwave or electromagnetic/thermal phnomena in food and materials processing: examples

Coupled electromagnetic/thermal systems

- Microwave heating
- Induction stirring and melting
- Magnetically-assisted single crystal growth in normal and microgravity
- Plasma processing
- Arc welding and vacuum refining
- Electromagnetic casting,
- Magnetic levitation, etc.

Basic concept of electromagnetic induction

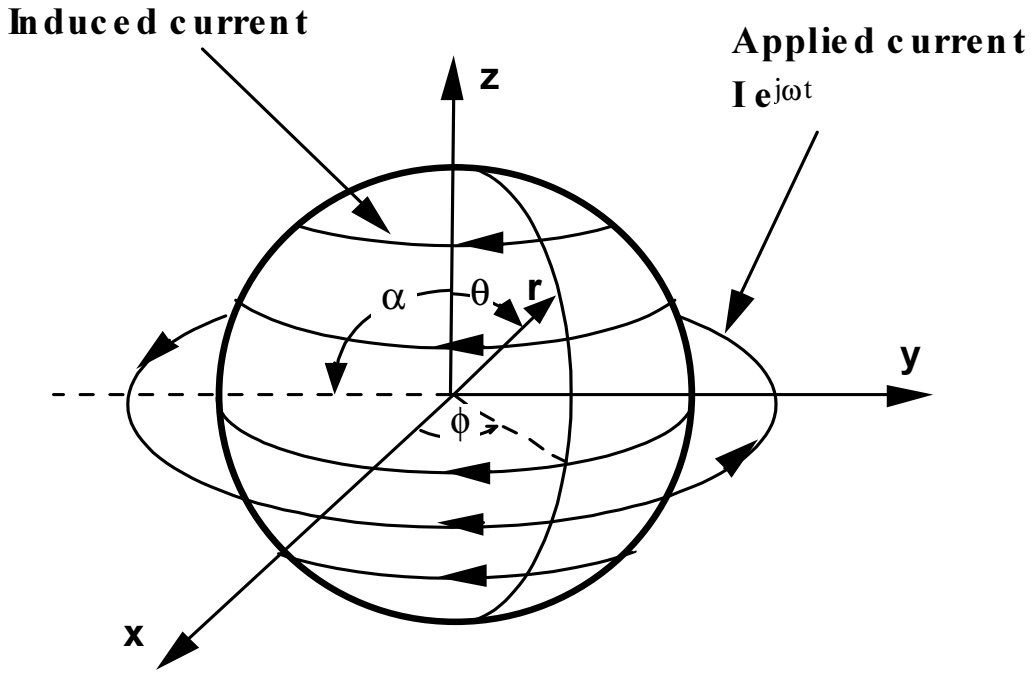

Microwave heating due to dipolar polarization

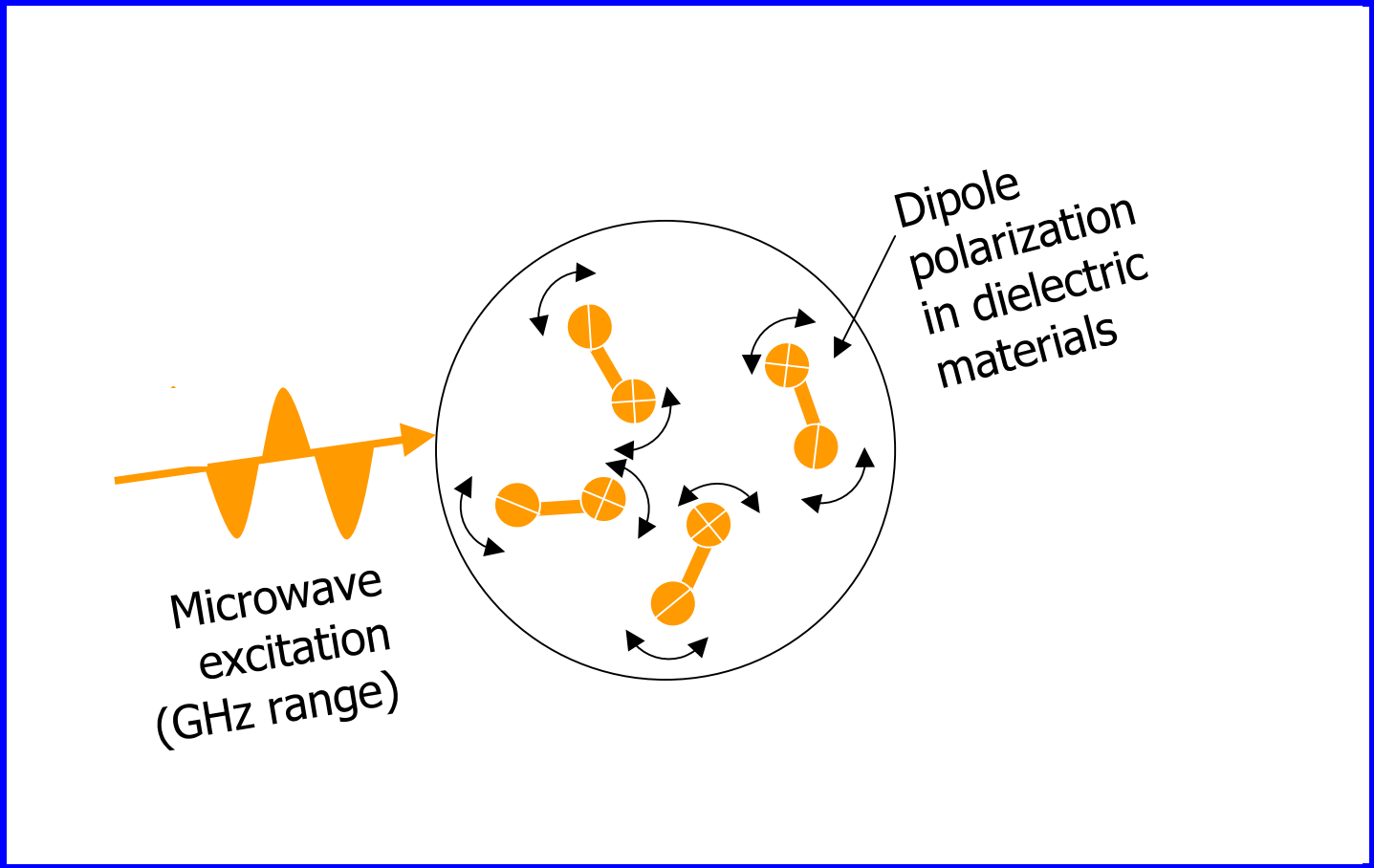

Mathematical formulation

$$\nabla \cdot \mathbf{D} = \rho_e$$

$$\nabla \times \mathbf{E} + \frac{\partial \mathbf{B}}{\partial t} = 0$$

$$\nabla \cdot \mathbf{B} = 0$$

$$\nabla \times \mathbf{H} = \mathbf{J} + \frac{\partial \mathbf{D}}{\partial t}$$

$$\mathbf{D} = \varepsilon \mathbf{E}$$

$$\mathbf{B} = \mu \mathbf{H}$$

Mathematical formulation(con't)

$\mathbf{J} = \sigma\left(\mathbf{E} + \mathbf{u} \times \mathbf{B}\right)$ *for moving frame (liquid metal)*

$\mathbf{J} = \mathrm{j}\omega\varepsilon_0 K\,\mathbf{E}$ *for conductor and dielectric solids*

$K_{metal} = -\mathrm{j}\sigma / \omega\varepsilon_0;$ $K_{dielectric} = \varepsilon' - \mathrm{j}\left(\sigma / \omega\varepsilon_0 + \varepsilon''\right)$

$$\rho C_p \frac{\partial T}{\partial t} + \rho C_p \mathbf{u} \cdot \nabla T = \nabla \cdot \kappa \nabla T + \mathbf{J} \cdot \mathbf{E}$$

$$\nabla \cdot \mathbf{u} = 0$$

$$\rho \frac{\partial \mathbf{u}}{\partial t} + \rho \mathbf{u} \cdot \nabla \mathbf{u} = -\nabla p + \nabla \cdot \eta\left(\nabla \mathbf{u} + \nabla \mathbf{u}^T\right) + \mathbf{J} \times \mathbf{B}$$

Mathematical formulation(con't)

- Boundary conditions for electromagnetic fields

$$\mathbf{D}_1 \cdot \mathbf{n} = \mathbf{D}_2 \cdot \mathbf{n} + \rho_s$$

$$\mathbf{E}_1 \times \mathbf{n} = \mathbf{E}_2 \times \mathbf{n}$$

$$\mathbf{B}_1 \cdot \mathbf{n} = \mathbf{B}_2 \cdot \mathbf{n}$$

$$\mathbf{H}_1 \times \mathbf{n} = \mathbf{H}_2 \times \mathbf{n} + \mathbf{J}_s$$

Mathematical formulation(con't)

- Boundary conditions for thermal problem

$$\frac{d\mathbf{X}}{dt} + \mathbf{u} \cdot \nabla \mathbf{X} = 0$$

$$\mathbf{n} \cdot \bar{\sigma} \cdot \mathbf{n} = 2\gamma H = -2\gamma \nabla \cdot \mathbf{n}$$

$$\mathbf{n} \cdot \bar{\sigma} \cdot \mathbf{t} = 0$$

$$-k\mathbf{n} \cdot \nabla T = \varepsilon \sigma_s \left(T^4 - T_\infty^4\right) + h\left(T - T_\infty\right)$$

Finite element fromulation for transport problems

$$\mathbf{M}\dot{\mathbf{U}}+\mathbf{K}(\mathbf{U})\mathbf{U}+\frac{1}{\varepsilon}\mathbf{C_P}\mathbf{M}_p\mathbf{C_P}^T\mathbf{U}+\mathbf{C_B}\mathbf{T}=\mathbf{F_U} \quad (flow)$$

$$\mathbf{M}_T\dot{\mathbf{T}}+\mathbf{K}_T(\mathbf{U})\mathbf{T}=\mathbf{F}_T \quad (thermal\ transport)$$

$$\mathbf{M}_C\dot{\mathbf{C}}+\mathbf{K}_C(\mathbf{U})\mathbf{C}=\mathbf{F}_C \quad (mass\ transport)$$

$$\mathbf{K}_\Phi\Phi+\mathbf{C}_\Phi\mathbf{U}=\mathbf{F}_\Phi \quad (magnetohydrodynamic\ effect)$$

Numerical solution for electromagnetic fields

- Finite element method
- Boundary element method (direct and indirect)
- Hybrid finite element/boundary element method
- Momemt, Time domain finite difference, etc.
- Analytical method

Finite element solution

Governing Equation

$$\nabla\times\frac{1}{\mathrm{j}\omega\mu}\nabla\times\mathbf{E}+\mathrm{j}\omega(\varepsilon+\mathrm{j}\sigma/\omega)\mathbf{E}=0$$

Finite element formulation

$$\iiint_{\Omega}\frac{1}{\mathrm{j}\omega\mu}\nabla\times\mathbf{E}\cdot\nabla\times\mathbf{E}\,d\Omega+\iiint_{\Omega}\mathrm{j}\omega(\varepsilon+\mathrm{j}\sigma/\omega)\mathbf{E}\cdot\mathbf{E}\,d\Omega$$

$$=\oint_{\partial\Omega}\mathbf{n}\times\mathbf{H}\cdot\mathbf{E}\,d\Gamma$$

$\nabla\cdot\varepsilon\mathbf{E}=0$ $\Leftarrow$ *ensured by the use of edge elements*

Boundary element solution

$$\nabla \times \frac{1}{\mathrm{j}\omega\mu} \nabla \times \mathbf{E} + \mathrm{j}\omega(\varepsilon + \mathrm{j}\sigma/\omega)\mathbf{E} = 0$$

$$\alpha_i \mathbf{E}_i = -\oint_{\partial\Omega} [\mathrm{j}\omega\mu \mathbf{n} \times \mathbf{H} \cdot G_i + \mathbf{n} \times \mathbf{E} \times \nabla G_i + \mathbf{n} \times \mathbf{E} \times \nabla G_i] d\Gamma$$

$$\nabla^2 G + \omega\mu(\varepsilon + \mathrm{j}\sigma/\omega) = -\delta(\mathbf{r} - \mathbf{r}_i)$$

Hybrid finite/boundary element solution

$$(\omega\varepsilon_1 + \mathrm{j}\sigma_1)\mathbf{E}_1 \cdot \mathbf{n} = (\omega\varepsilon_1 + \mathrm{j}\sigma_1)\mathbf{E}_2 \cdot \mathbf{n}$$

$$\mathbf{E}_1 \times \mathbf{n} = \mathbf{E}_2 \times \mathbf{n}$$

$$\mu_1\mathbf{H}_1 \cdot \mathbf{n} = \mu_2\mathbf{H}_2 \cdot \mathbf{n}$$

$$\mathbf{H}_1 \times \mathbf{n} = \mathbf{H}_2 \times \mathbf{n}$$

Comparison: Advatanges and disadvantages

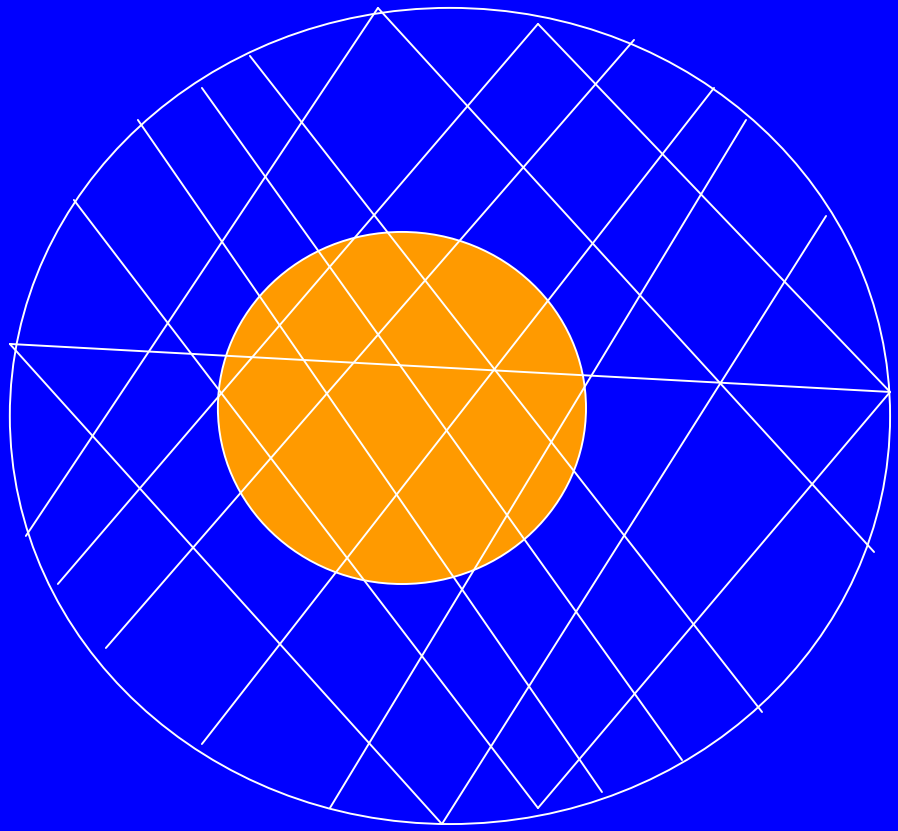

FE

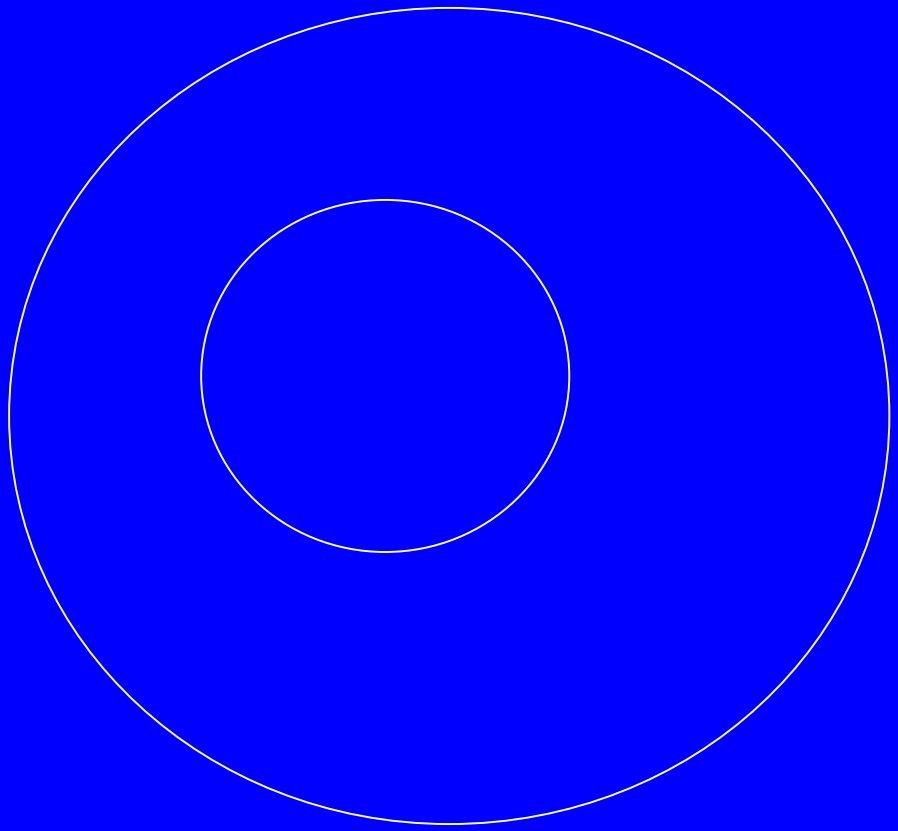

BE

Advatanges and disadvantages (Continued)

	FE	BE	FBE
Mesh	Volume including free space	Surface	Volume in region of concern & surface outside
Mesh points	N_{FE}^{3}	N_{BE}^{2}	between
Open boundary condition	Artificial boundaries	Automatically satisfied	Automatically satisfied
Non-linearity	Easy to treat	Cumbersome or difficult to treat	Easy to treat
Matrix structure	Sparse matrix	Full matrix	Largely sparse
Solution time	$N_{FE}^{3.5 \text{ to } 4.5}$	N_{BE}^{6}	Between

Parallel computation

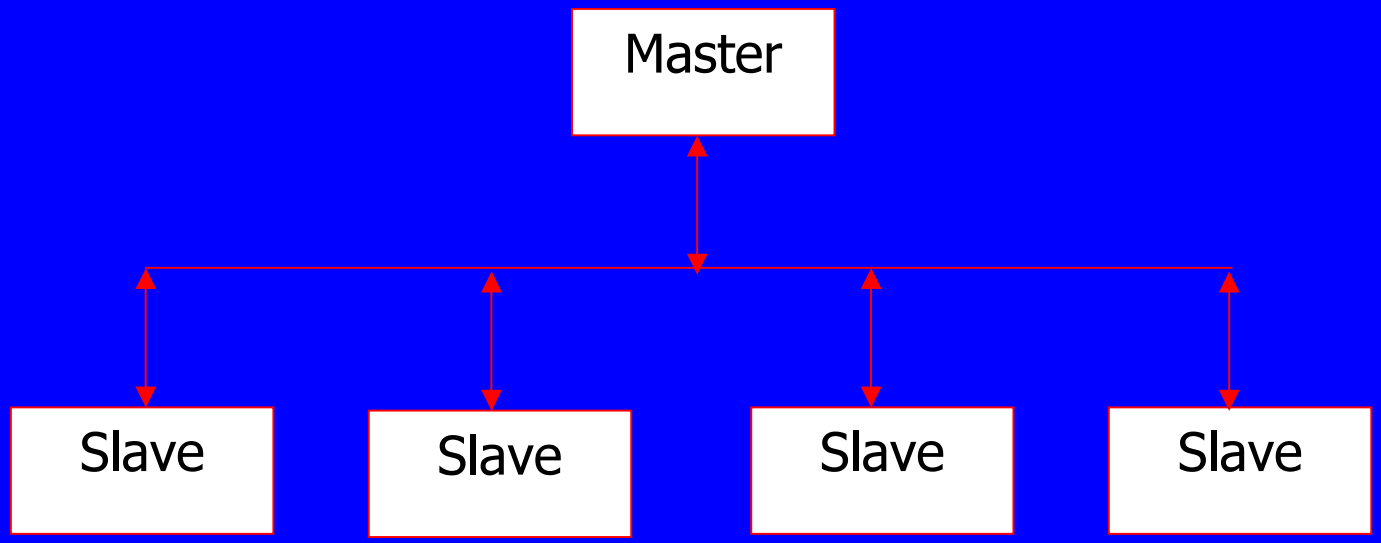

Parallel computing

Master Program

start velocity field calculations
create slave tasks
distribute slave tasks
receive data from slaves
update field
repeat process (2)-(5) until
the calculation is
complete

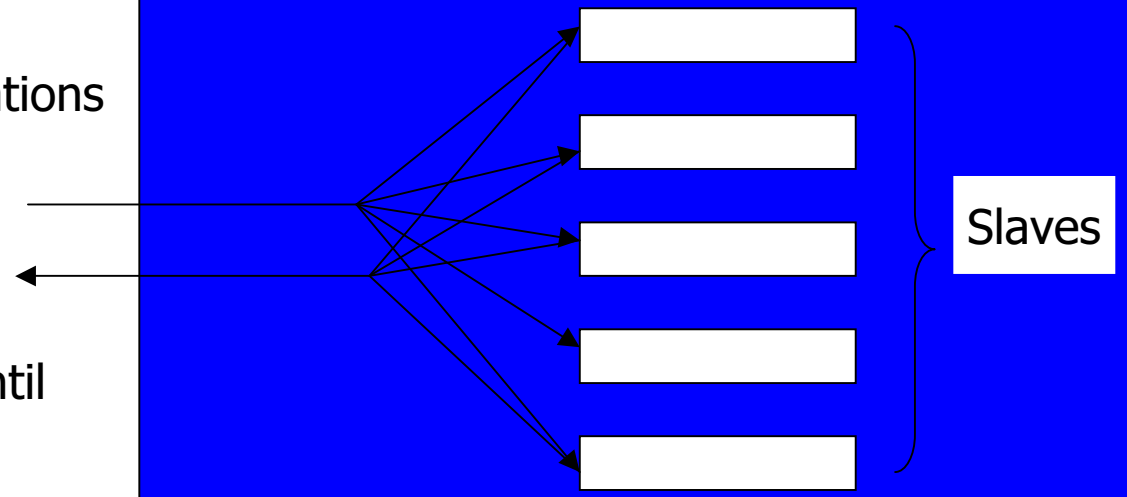

Parallel computing

Slave Program

receive data for setting up problem

calculate data of FE or BE elements

send data to master

Matrix blocks

exit

Parallel computing

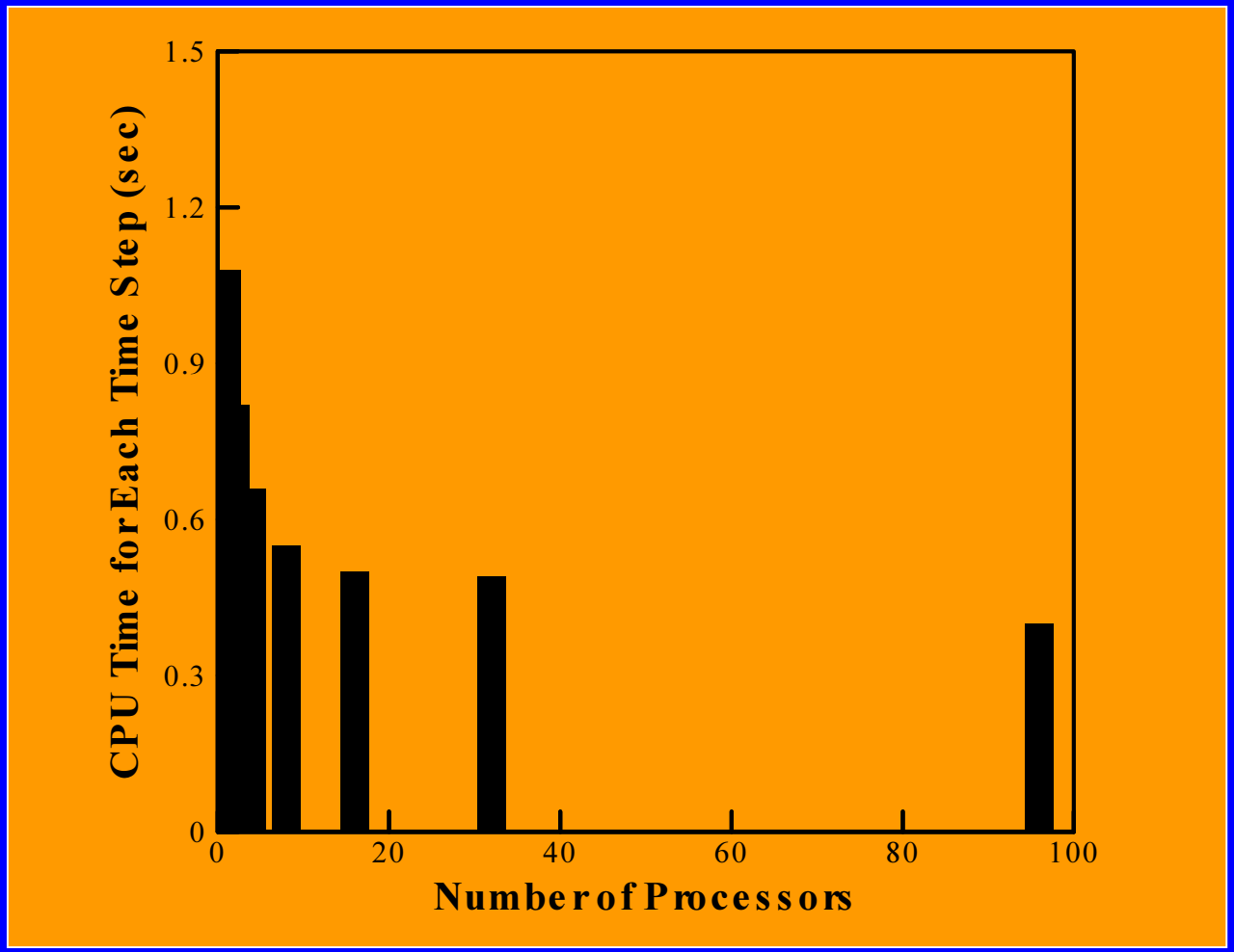

RESULTS

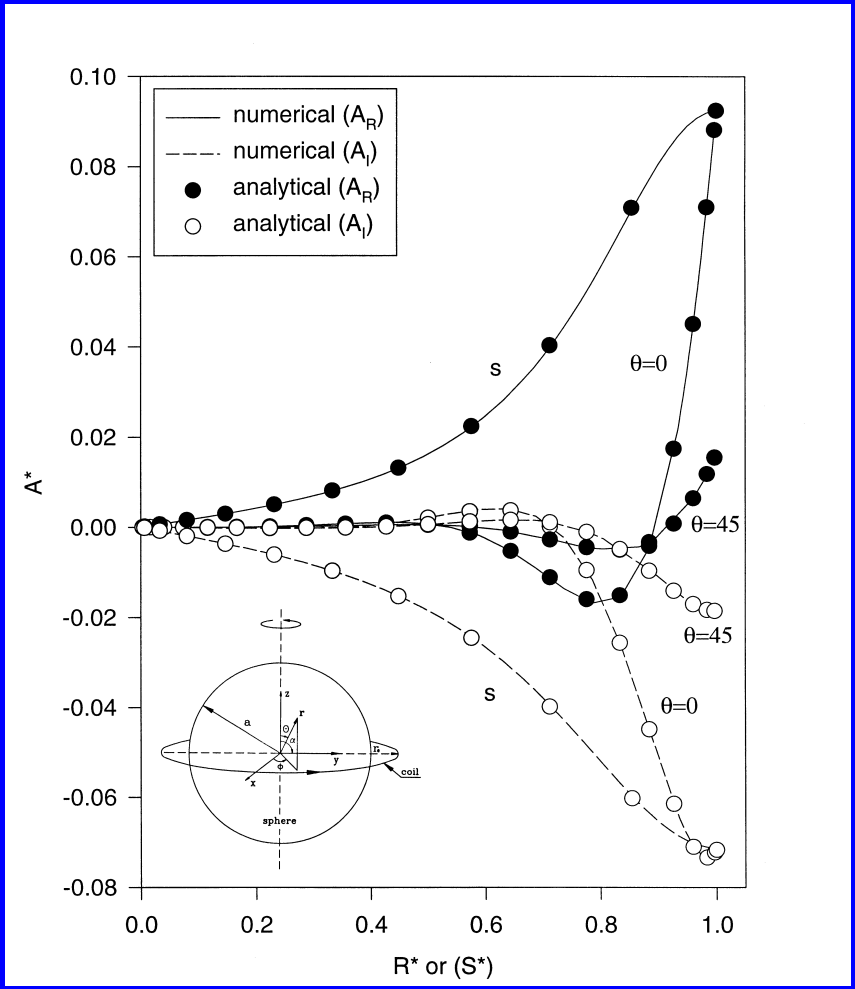

Comparison of numerical and analytical results for the radial and surface distribution of the vector potential at different θ angles.

Magnetic levitation

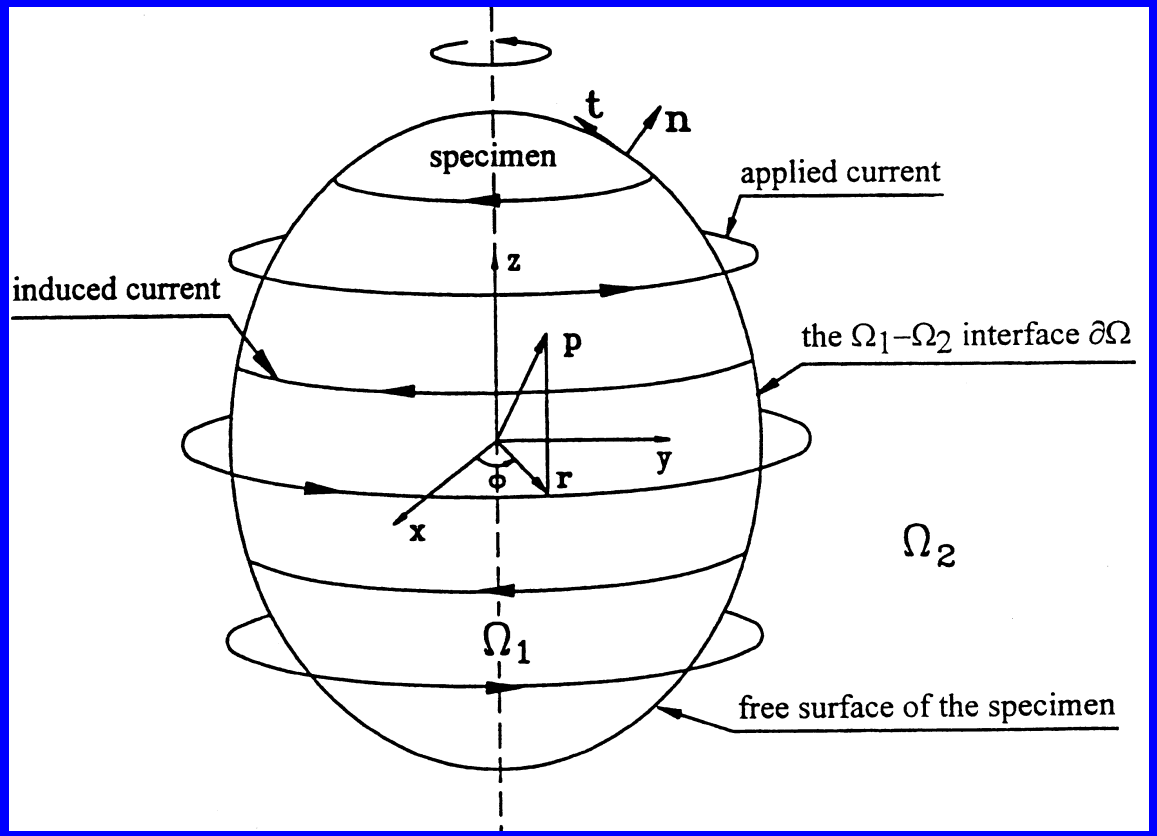

Coordinate systems and FEM and BEM domains used for calcualtions.

- FEM formulation for Magnetic Vector Potential:

$$\int_{\partial\Omega_1} r\frac{\partial A}{\partial n}\psi_i d\Gamma - \int_{\Omega_1} r\left(\nabla A \bullet \nabla \psi_i + \frac{1}{r^2} A\psi_i + k^2 A\psi_i\right) d\Omega = 0$$

$$\mathbf{KA} + \mathbf{N_I q_I} = 0$$

- BEM Formulation for Magnetic Vector Potential:

$$\frac{1}{2\pi} C(\mathbf{r}_i) A(\mathbf{r}_i) + \oint_{\partial\Omega_2} A(\mathbf{n} \bullet \nabla G) r d\Gamma + \oint_{\partial\overline{\Omega}_2} A(\mathbf{n} \bullet \nabla G) r d\Gamma =$$

$$\oint_{\partial\Omega_2} G(\mathbf{n} \bullet \nabla A) r d\Gamma + \oint_{\partial\overline{\Omega}_2} G(\mathbf{n} \bullet \nabla A) r d\Gamma + \int_{\Omega_2} \mu J G r d\Omega$$

$$\mathbf{HA_I} = \mathbf{Gq_I} + \mathbf{F}$$

- coupling of boundary and finite elements

$$\begin{bmatrix}\mathbf{H}_I & \mathbf{H}_B\end{bmatrix}\begin{Bmatrix}\mathbf{A}_I \\ \mathbf{A}_B\end{Bmatrix} = \begin{bmatrix}\mathbf{G}_I & \mathbf{G}_B\end{bmatrix}\begin{Bmatrix}\mathbf{q}_I \\ \mathbf{q}_B\end{Bmatrix} + \begin{Bmatrix}\mathbf{F}_I \\ \mathbf{F}_B\end{Bmatrix}$$

$$\mathbf{q}_I = \mathbf{M}\mathbf{A}_I + \mathbf{F}'$$

$$\overline{\mathbf{K}}\,\overline{\mathbf{A}} = \overline{\mathbf{F}}$$

Analytical solutions & asymptotic behavior

$$J_\phi = -\frac{j\omega\mu I \sin\alpha}{2}\left(\frac{a}{r}\right)^{1/2}\sum_{n=1}^{\infty}\frac{2n+1}{n(n+1)}\left(\frac{a}{r_o}\right)^{n}\frac{P_n^1(\cos\alpha)P_n^1(\cos\theta)I_{n+1/2}(kr)}{kaI_{n-1/2}(ka)}$$

$$I_\nu(x) \xrightarrow[\infty]{} \frac{e^x}{\sqrt{x}}$$

$$J_\phi \propto e^{-(a-r)/\delta}$$

$$Q_{tot} \propto I^2\sqrt{\frac{\mu\omega}{\sigma}}\ as\ \omega \to \infty$$

$$T(r,\theta) \propto I^2\sqrt{\frac{\mu\omega}{\sigma}}\ as\ \omega \to \infty$$

Comparison between numerical and analytical solutions

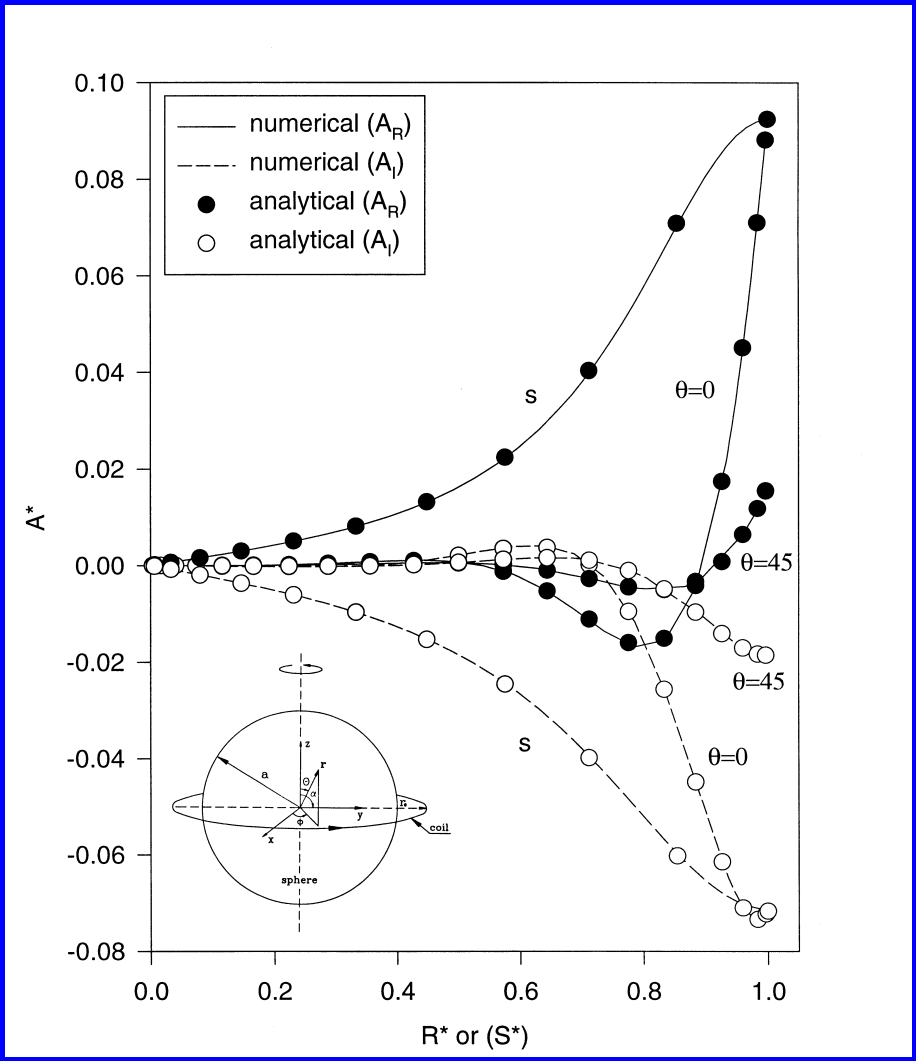

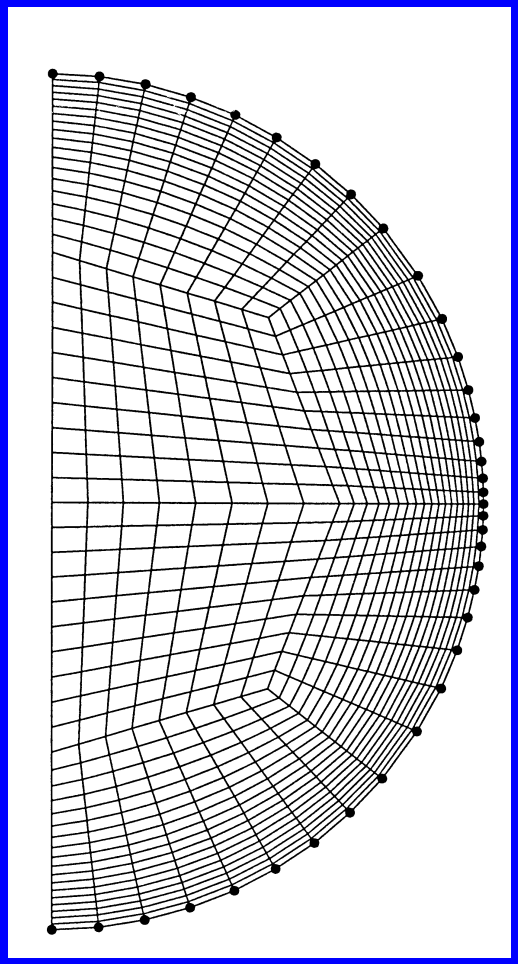

$N_{BE}=37$

$N_{FE}=288 \times 2$

Finite element and boundary element meshes used for eletromagnetic, fluid flow and heat transfer calculations.

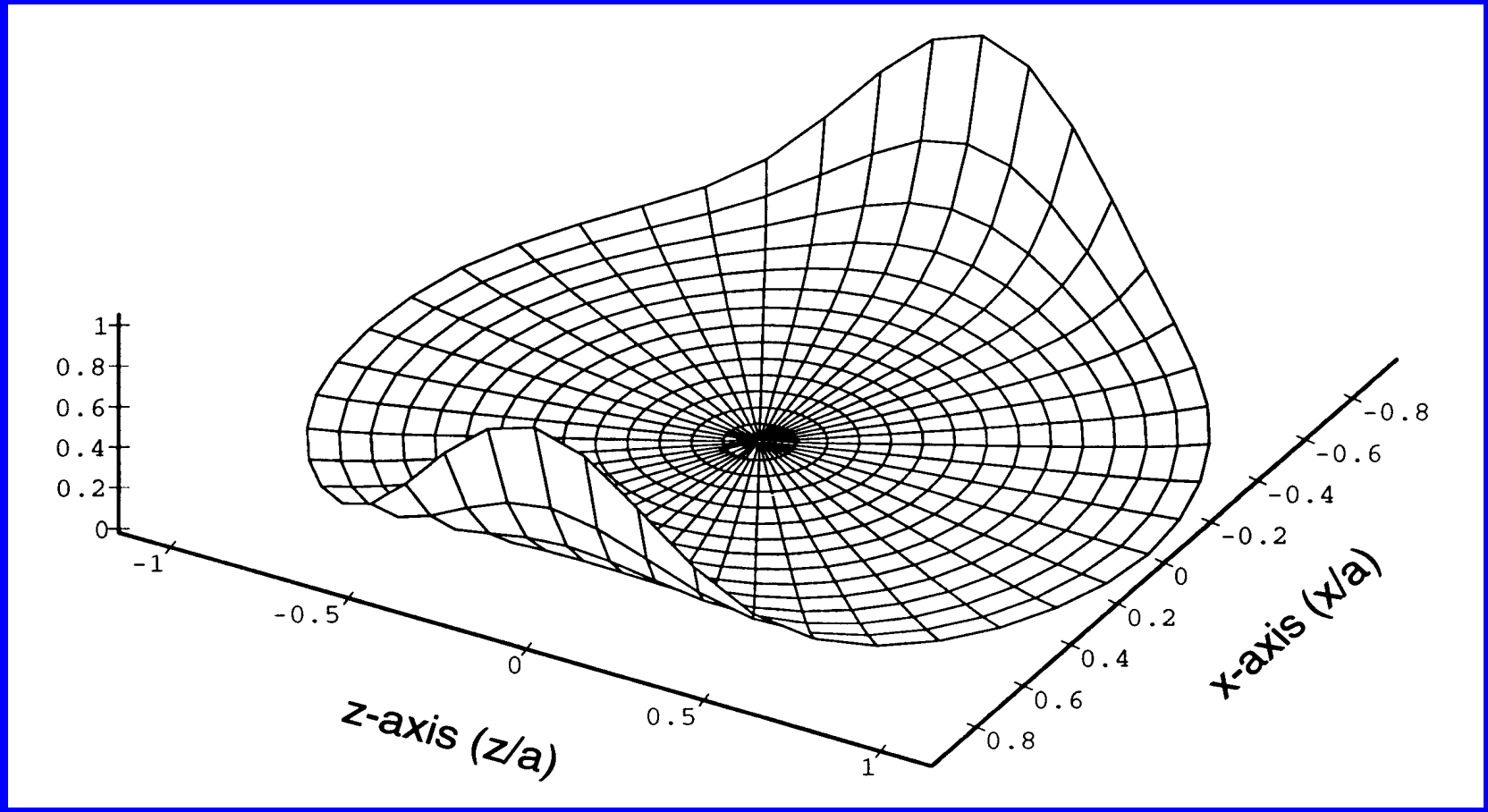

Three-D view of the Joule heating distribution within the cross section of a deformed conducting sphere, cut through z-axis. The vertical axis is the nondimensionalized Joule heating distribution, $Q^*(r,\theta) = 16a^2 Q(r,\theta)/\mu\omega I^2$

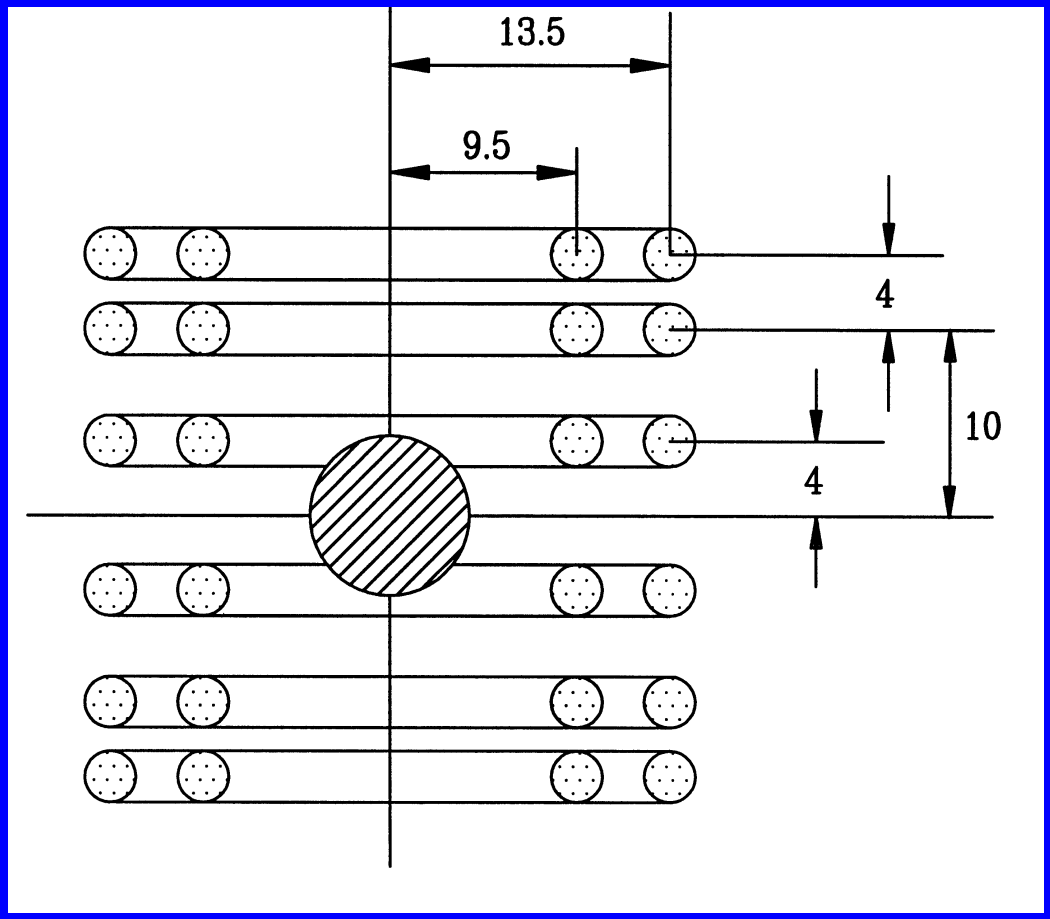

Schematic representation of TEMPUS for microgravity applications: the inner four coils are for heating and sample squeezing and the outer eight coils are for positioning.

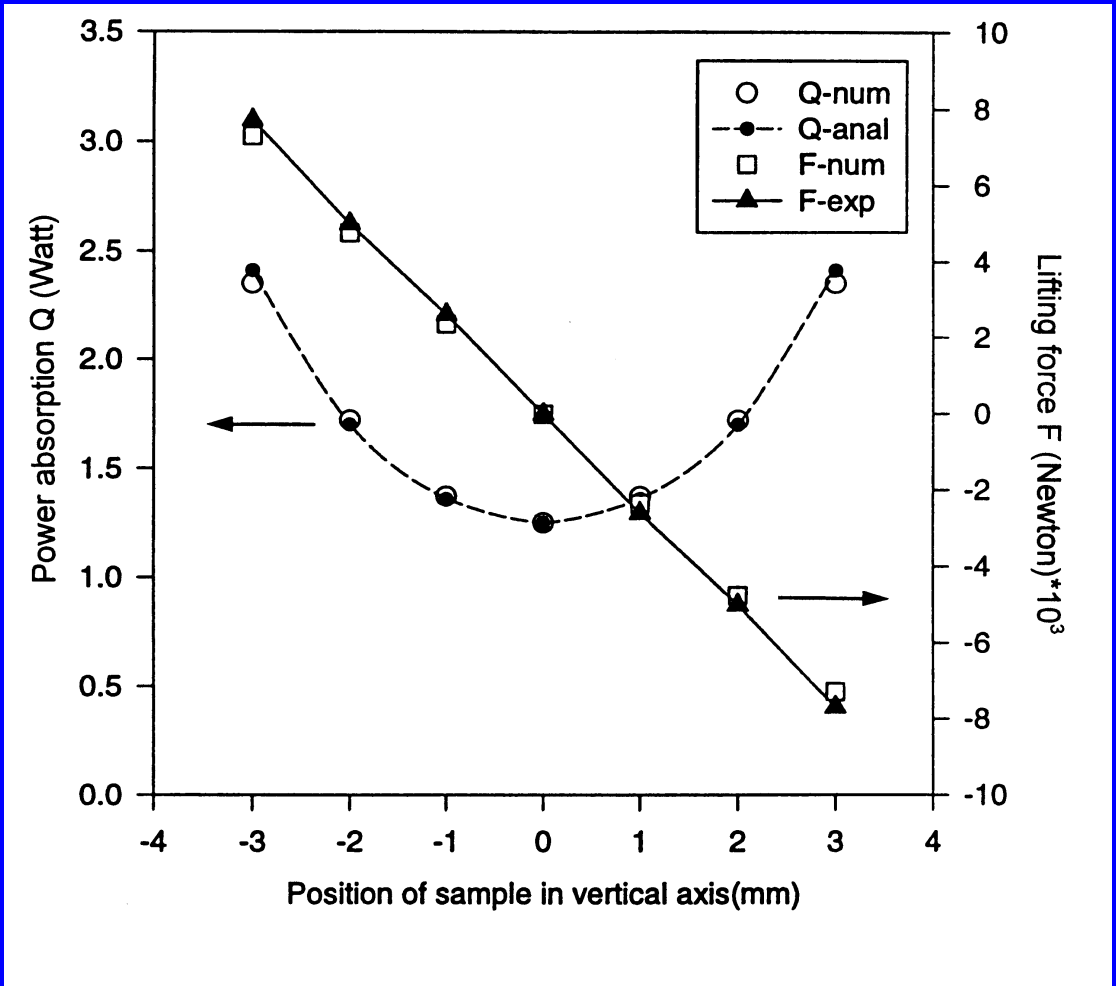

Numerical, analytical and experimental results of lifting force on and power absorption in a 10 mm diameter copper sphere induced by TEMPUS positioning coils only according to the sample positions along the vertical axis

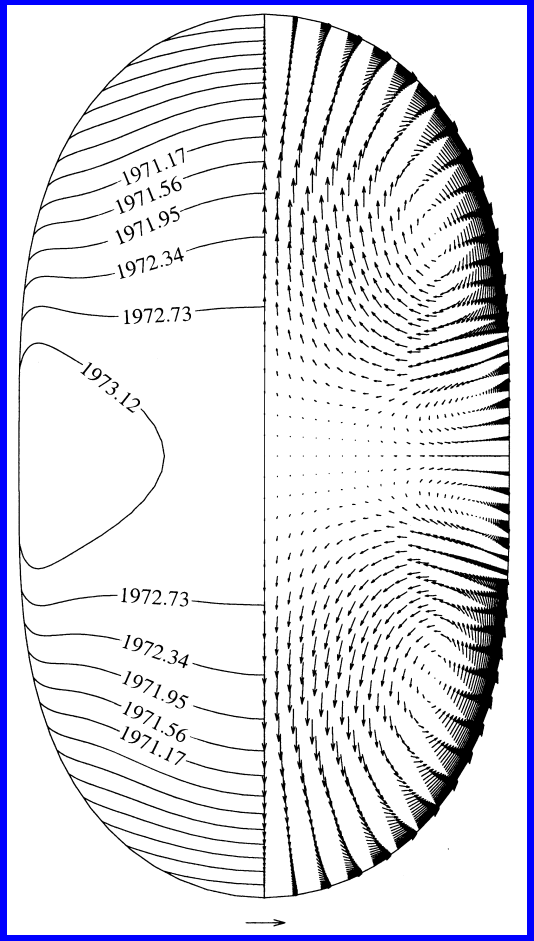

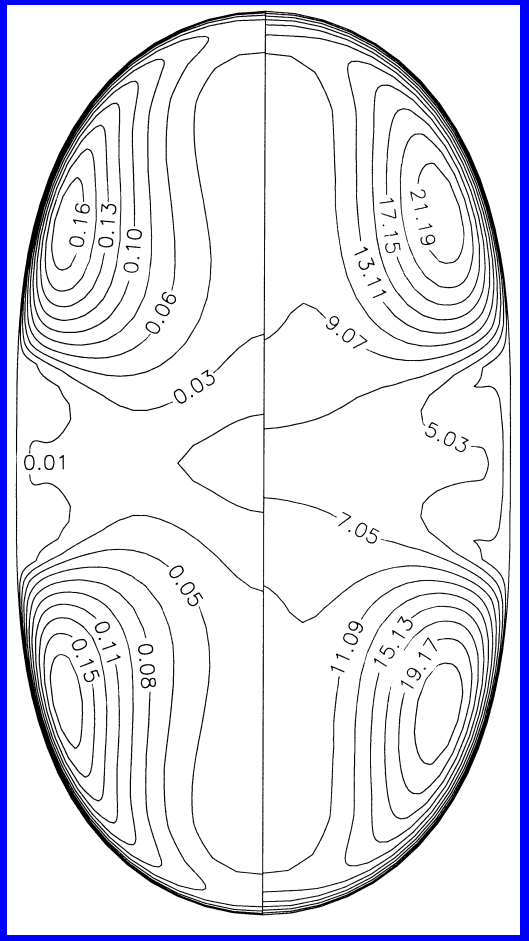

Distribution of turbulent velocity (left-right), temperature dis field(left-left), turbulent kinetic energy (right-left) and ratio of effective viscosity to molecular viscosity (right-right) in a silver droplet in TEMPUS device during space flight. Maximum velocity=14 cm/s and temperature is in K.

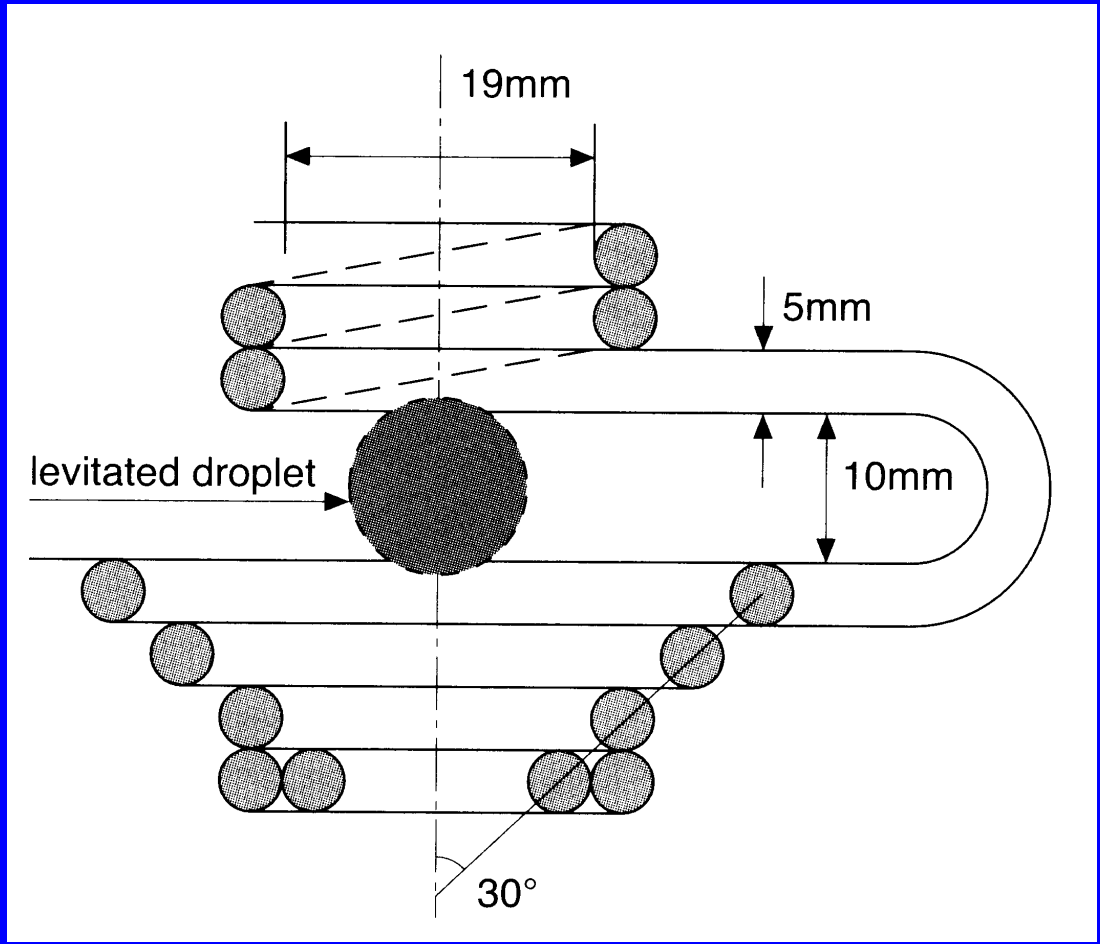

The configuration and dimensions of the coils used for magnetic levitation under terrestrial conditions.

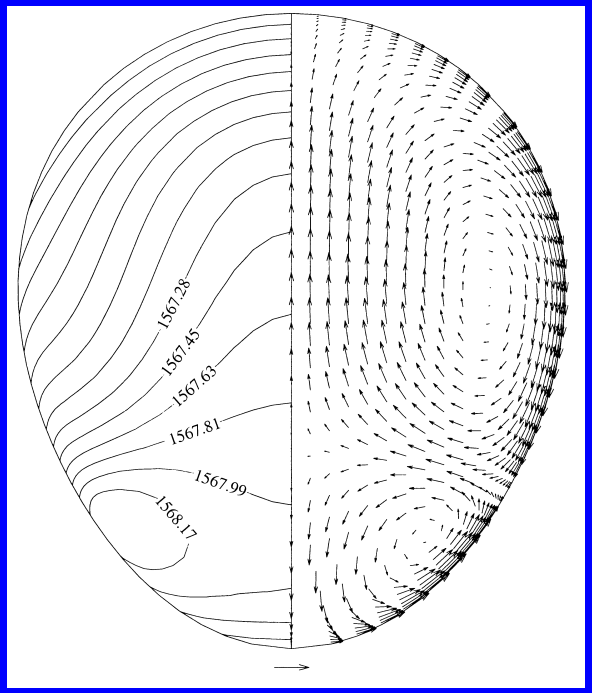

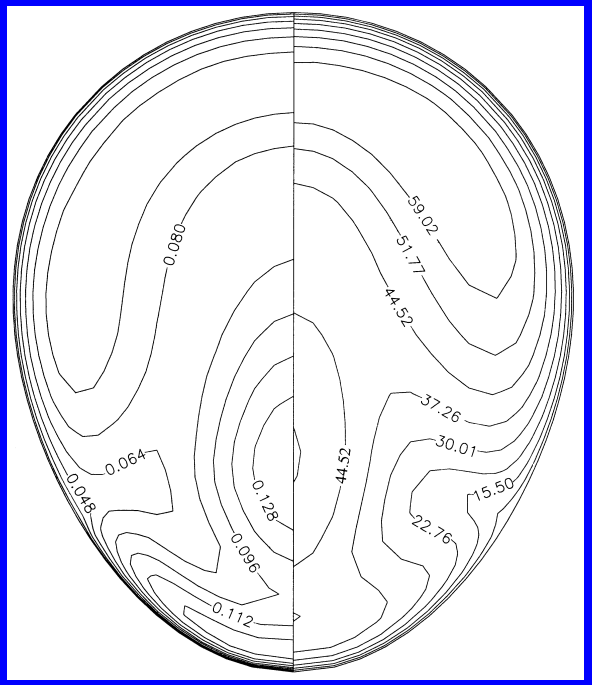

Surface deformation and the distribution of turbulent velocity U_{max}=21 cm/s) and temperature (left-left, in K), turbulent kinetic energy and turbulent-melocular viscosity ratio (max=66.5) in a magnetically-positioned aluminum droplet (10 mm initial diameter) in normal-gravity condition.

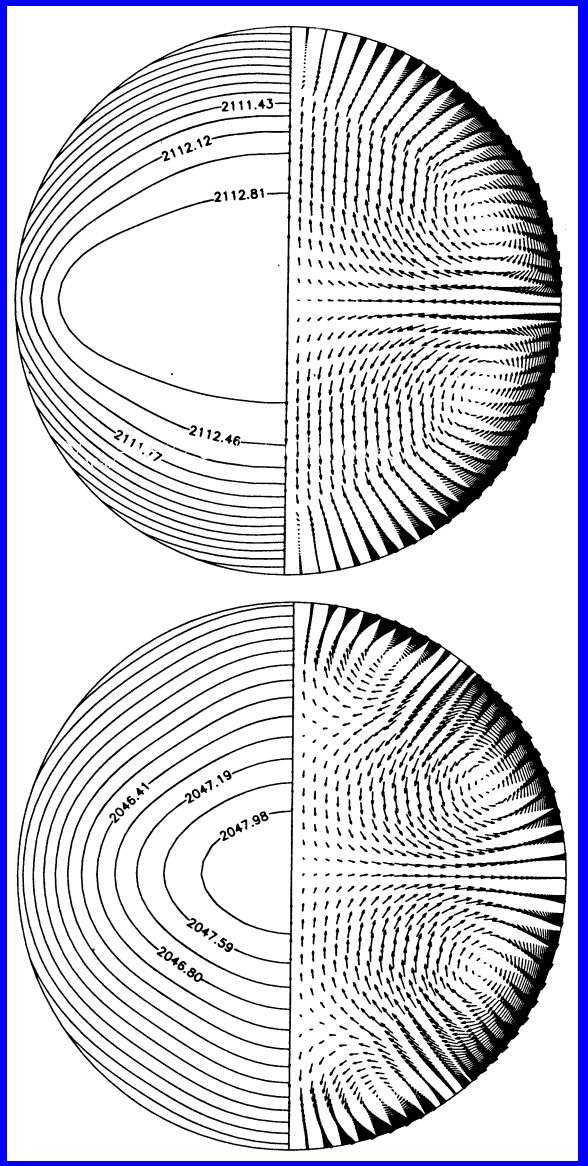

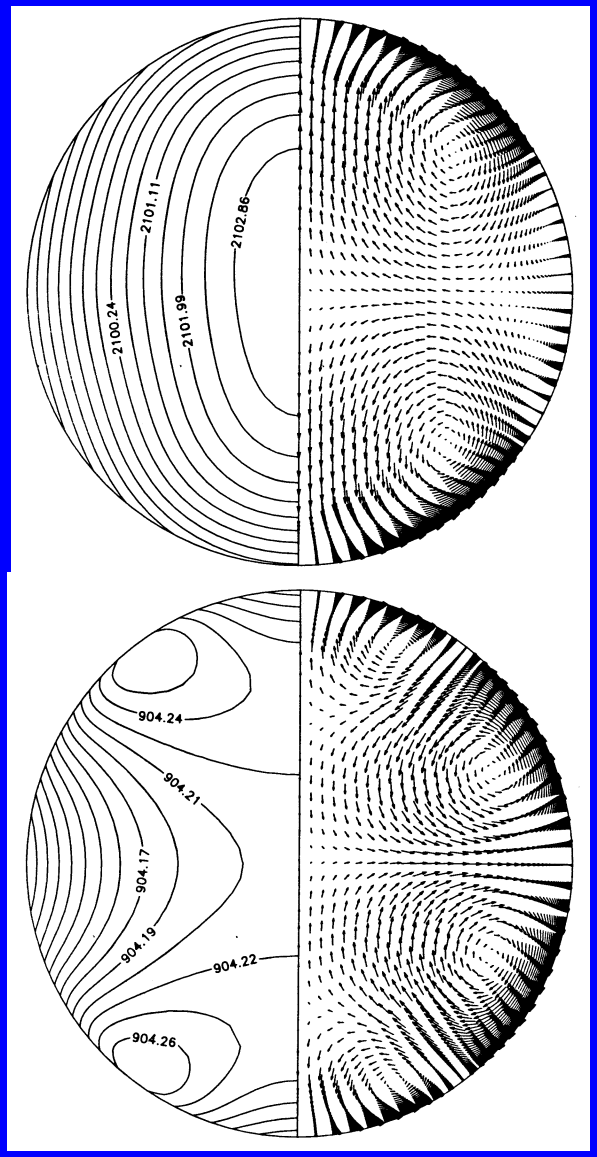

Transient response of thermal and fluid flow filed to the change in magnetic fields

Droplet oscillation over a period

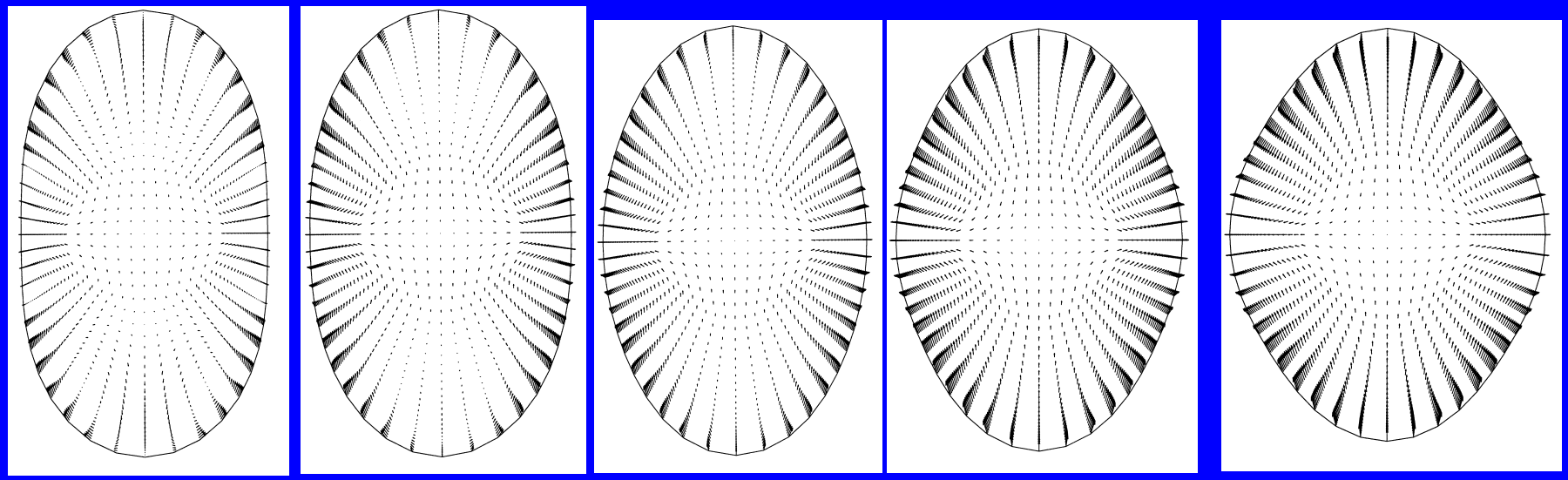

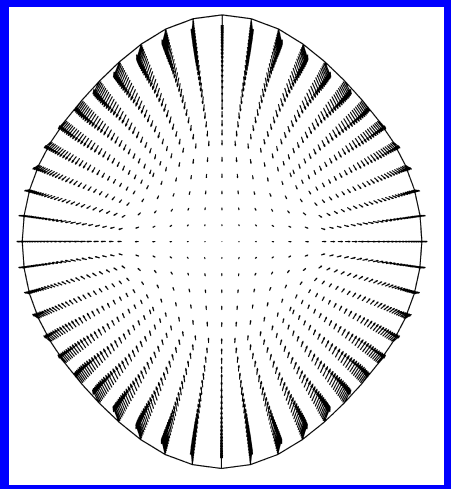

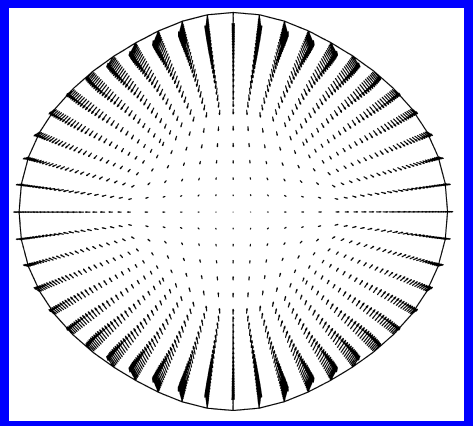

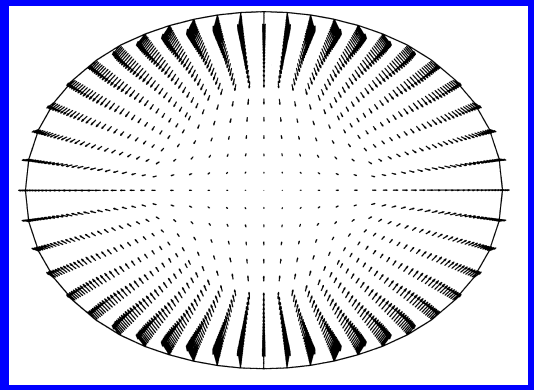

Droplet oscillation(con't)

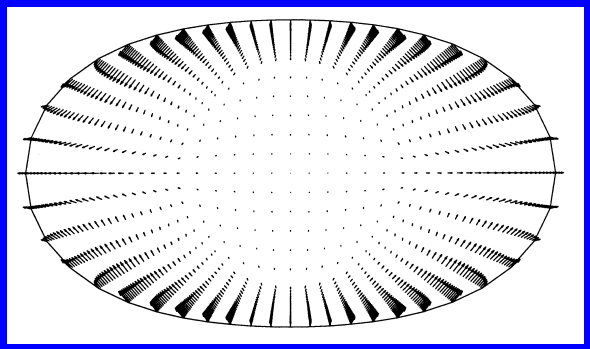

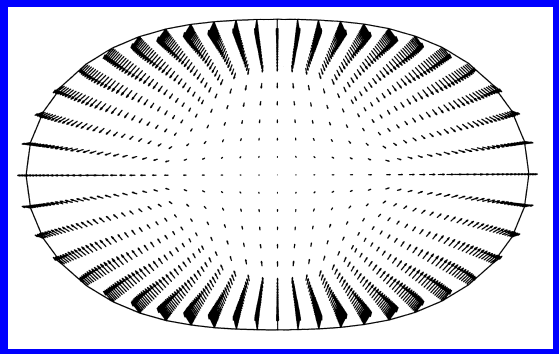

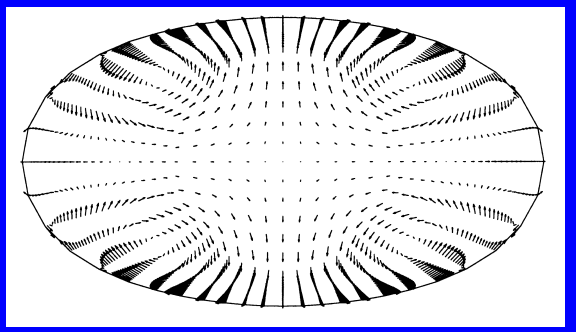

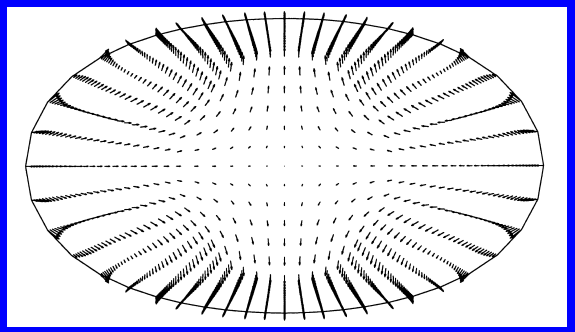

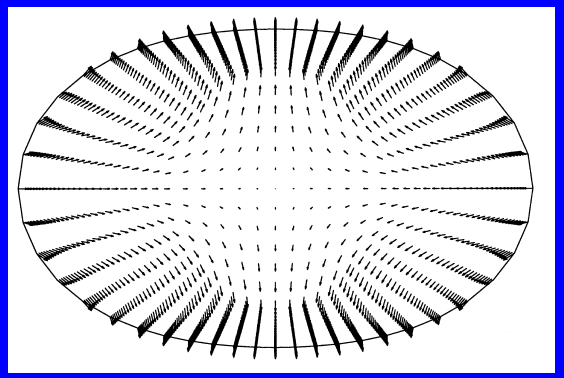

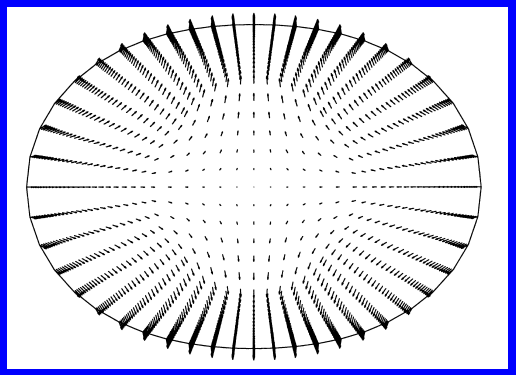

Droplet oscillation(con't)

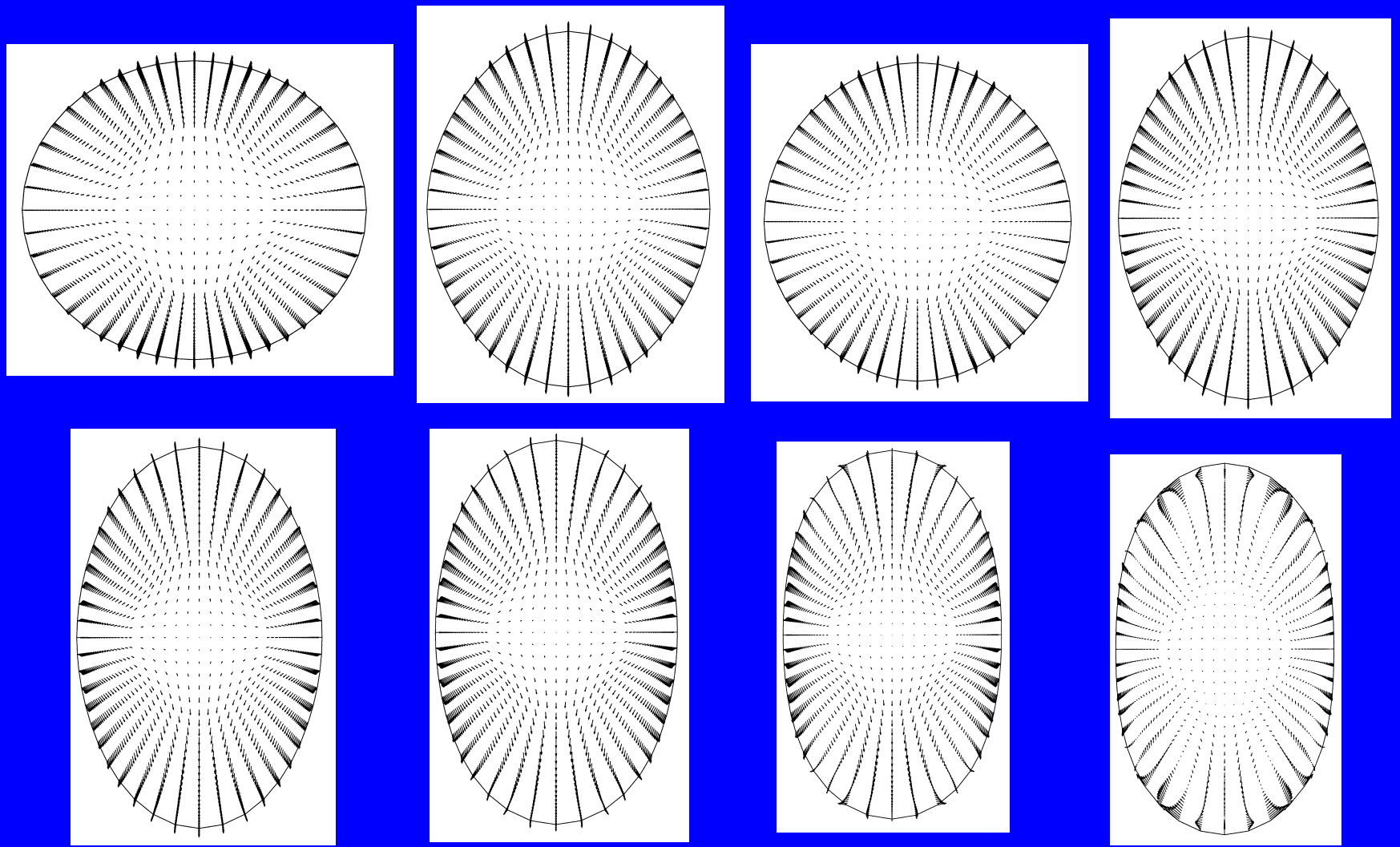

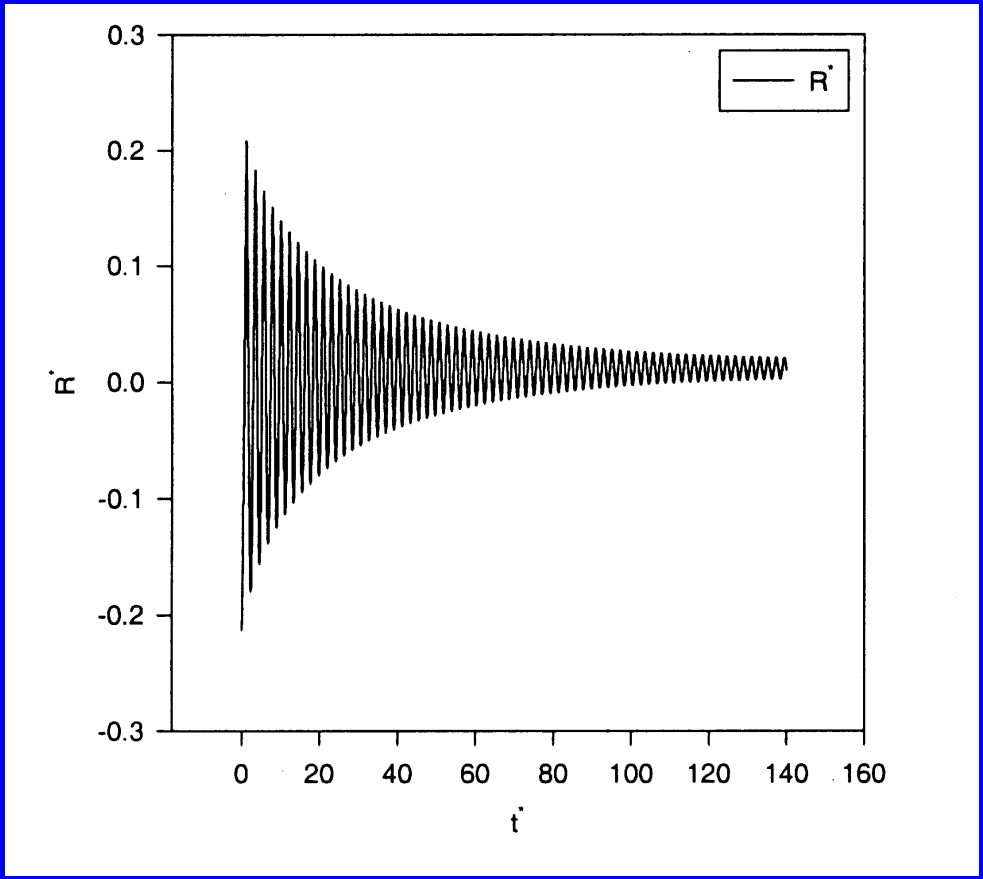

History of R_o^* = $(R(z=0,t)-R_0/R_0)$ with positioning coils on.

Electromagnetic casting

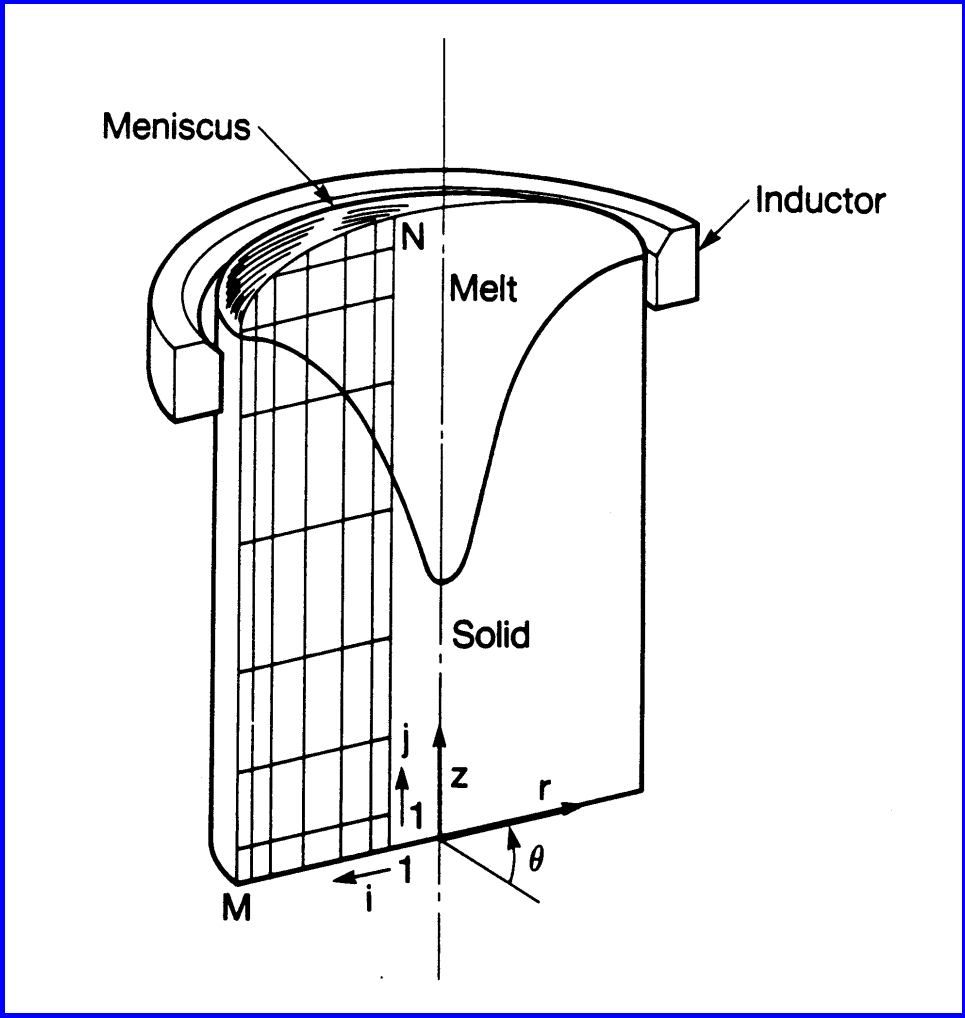

Comparison of numerical & experimental results

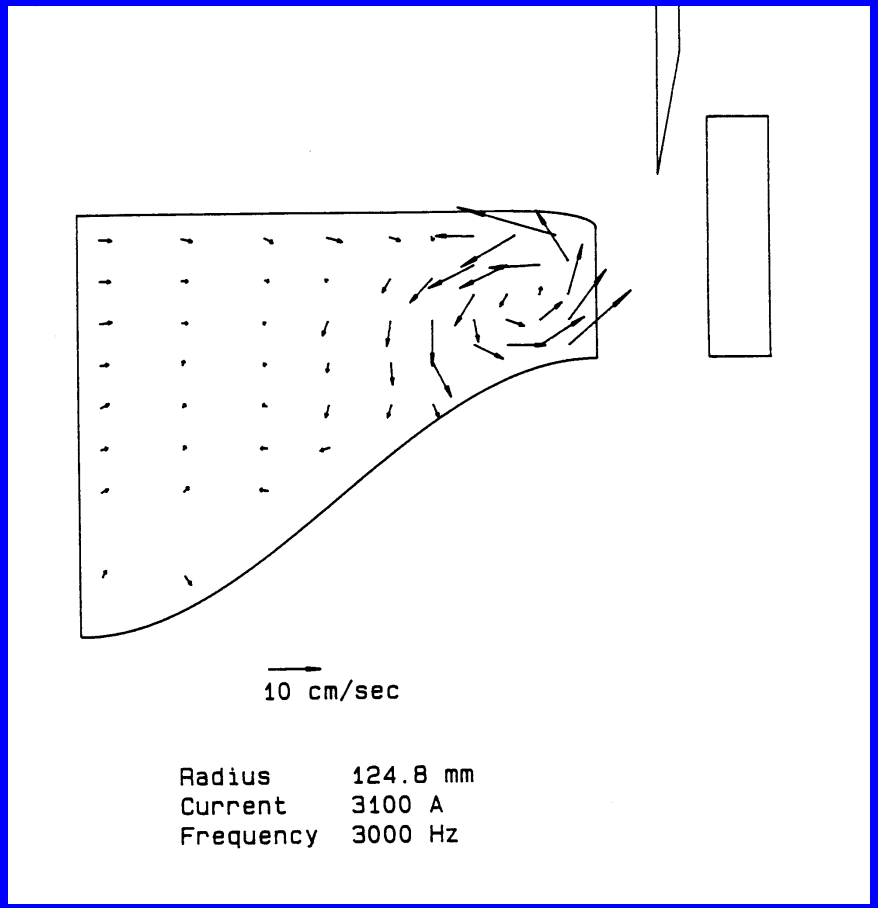

Numerical

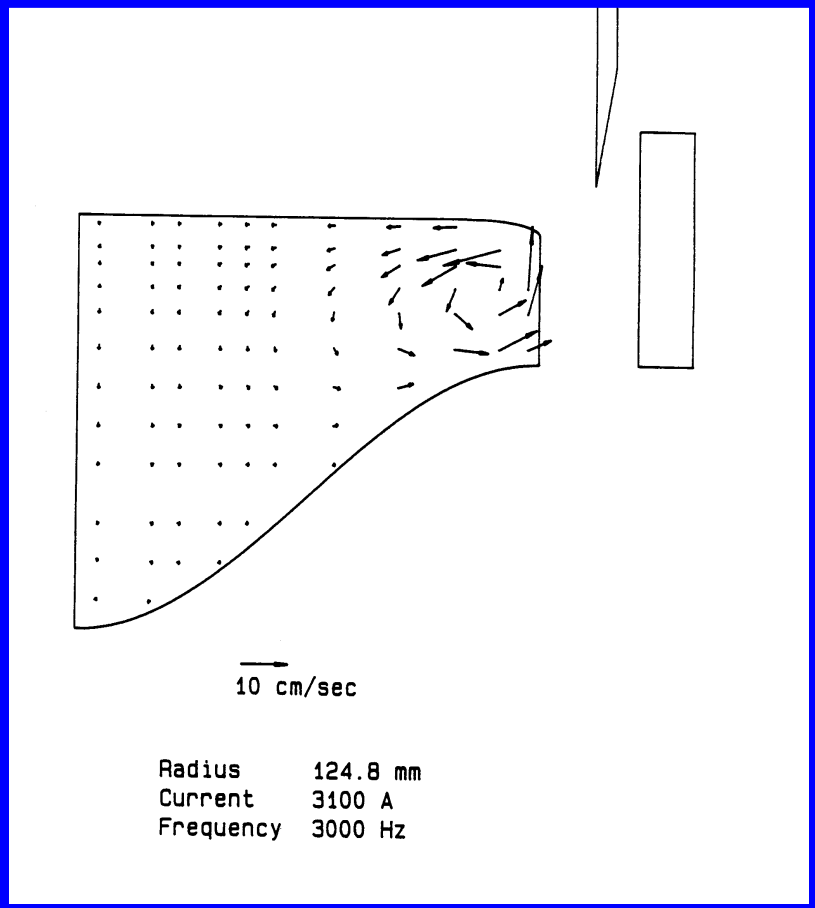

Experimental

3-D electromagnetic field & melt meniscii

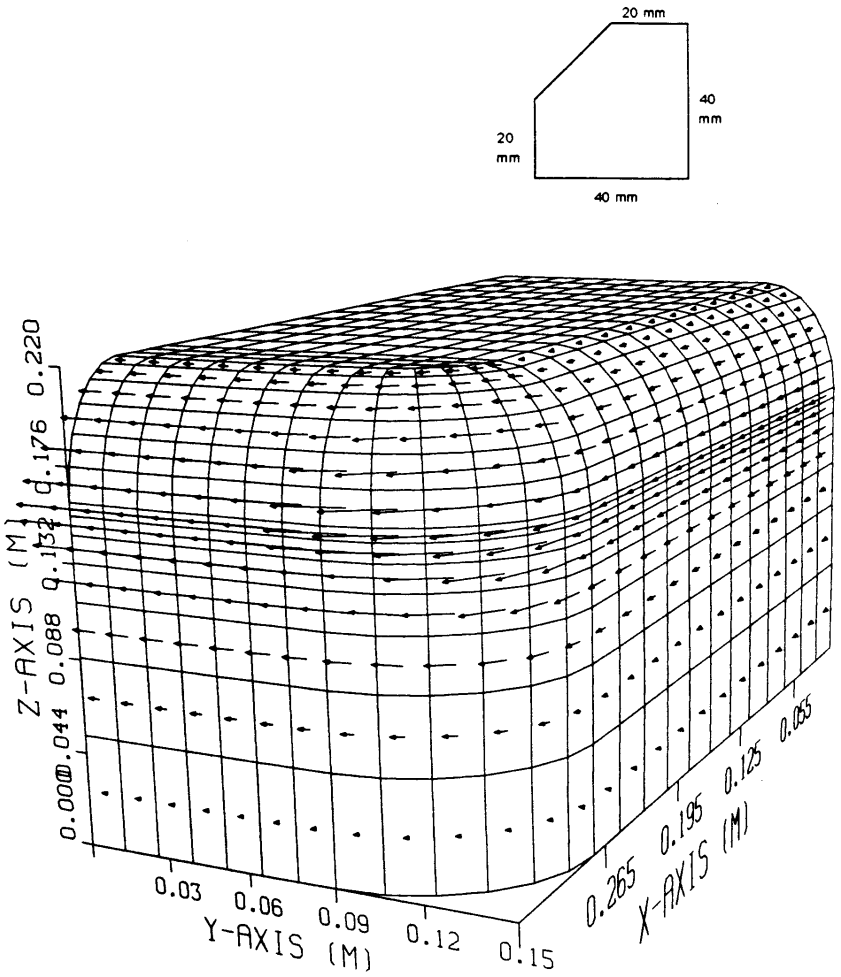

Electromagnetic stirring

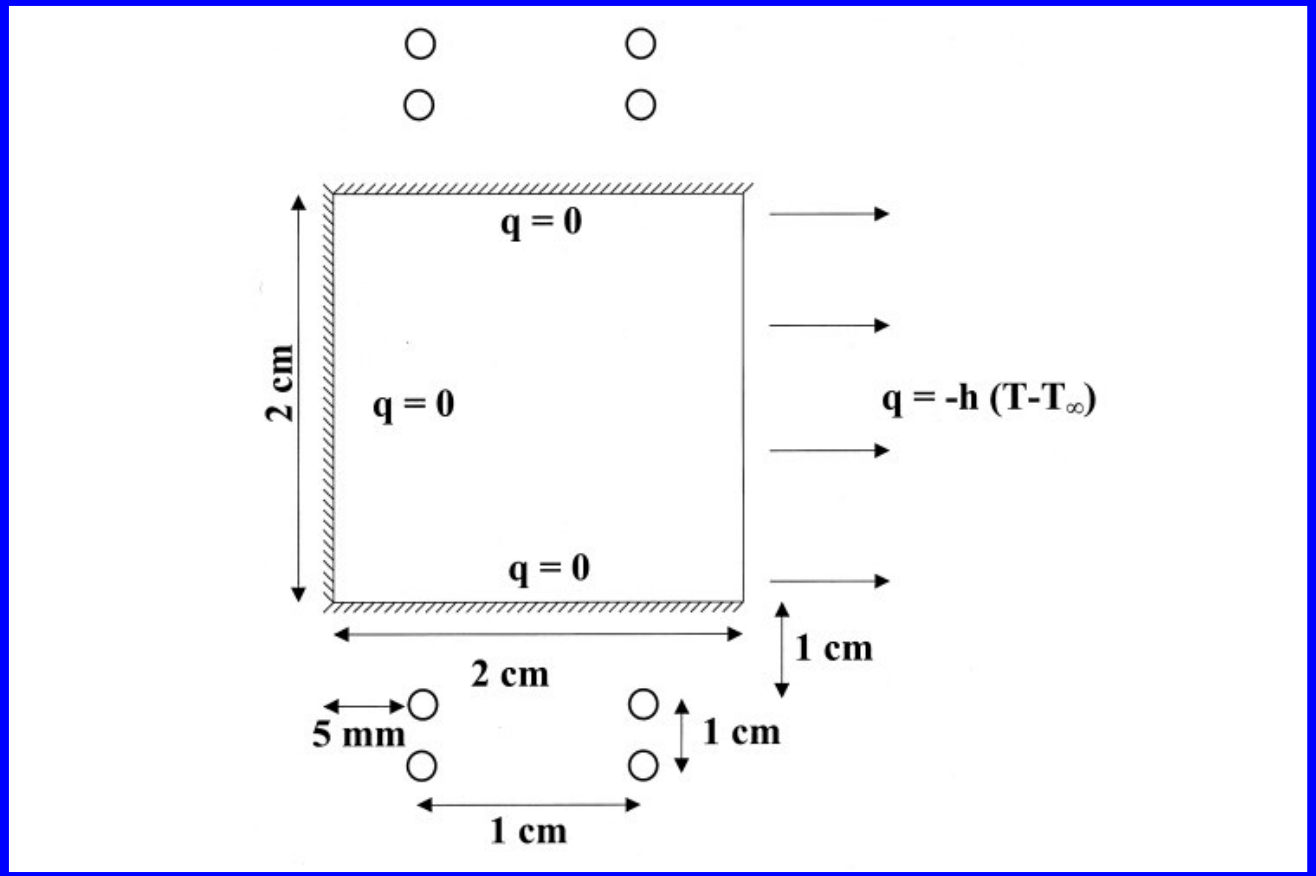

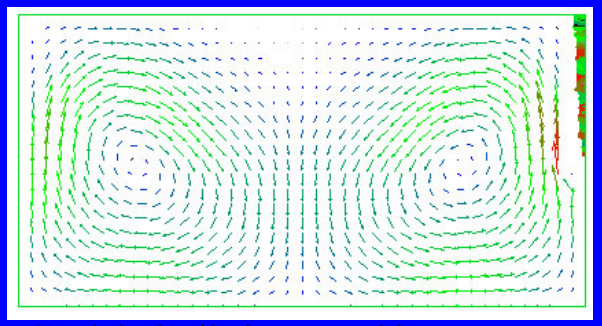

(a): Velocity plot with microstructure: t 0.65s; Max velocity = 0.021 m/s; Re = 342.72

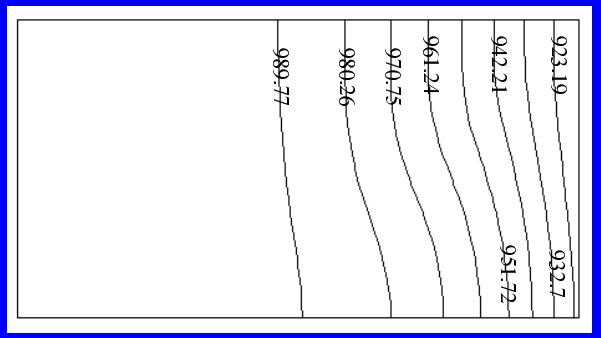

(b): Temperature contour plot at t = 0.65 s

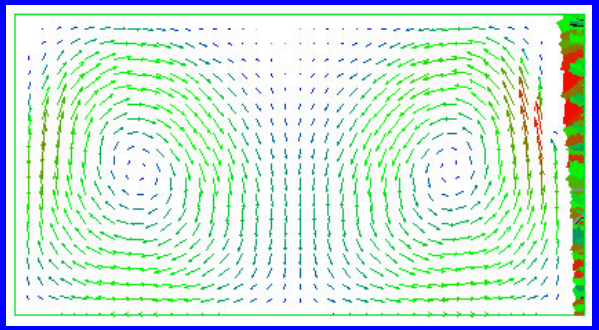

(c): Velocity plot with microstructure: t = 0.95s; Max velocity = 0.023 m/s; Re = 375.36

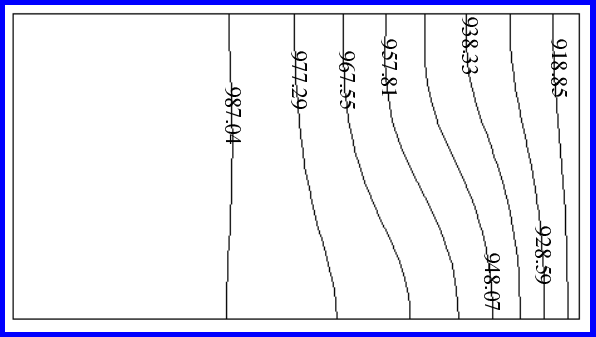

(d): Temperature contour plot at t = 0.95 s

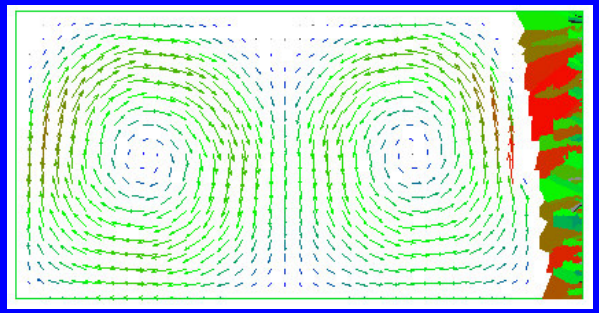

(e): Velocity plot with microstructure: t=1.75s; Max velocity = 0.03 m/s; Re = 489.6

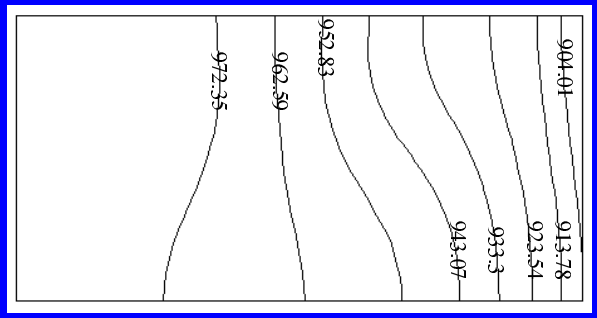

(f): Temperature contour plot at t = 1.75 s

Flow and microstructure evolution (vedio)

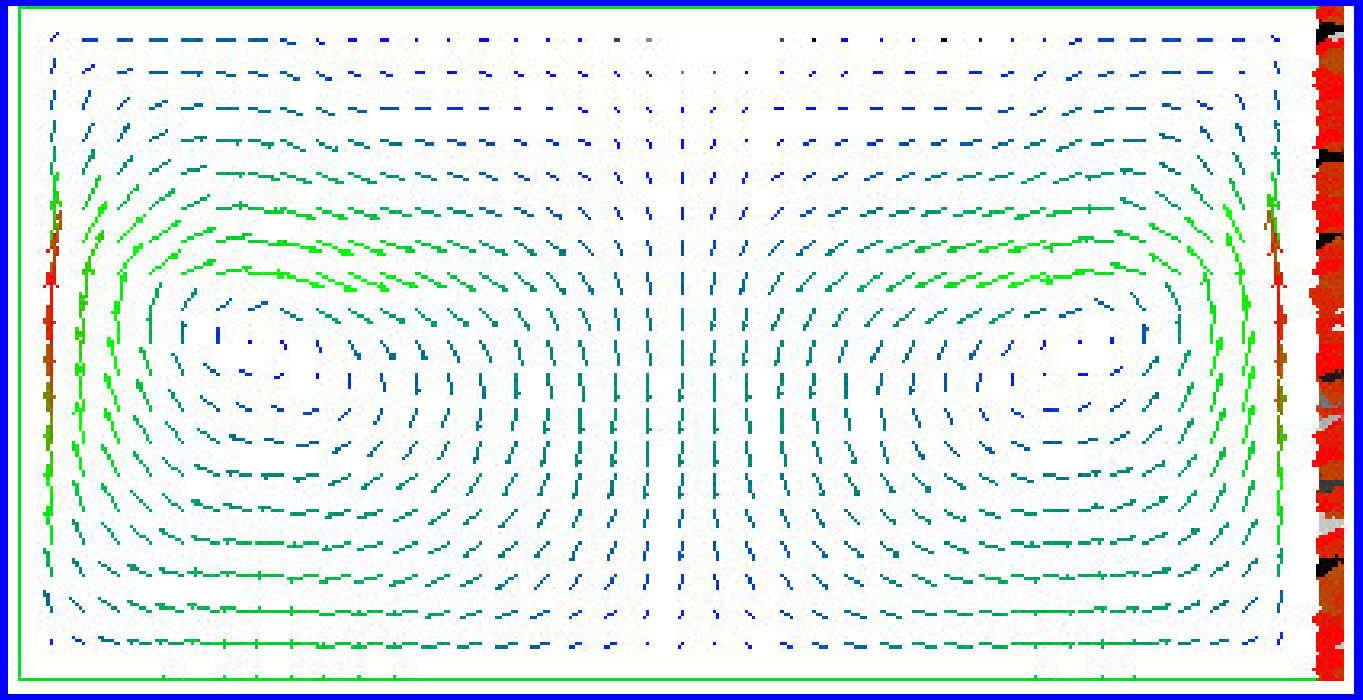

Crystal growth in magnetic fields

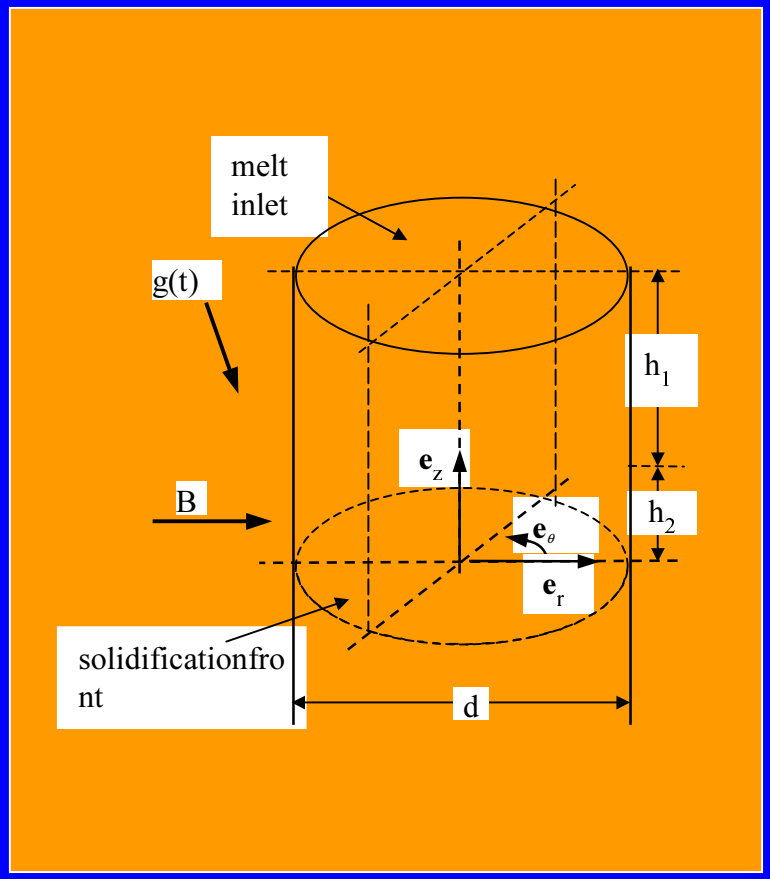

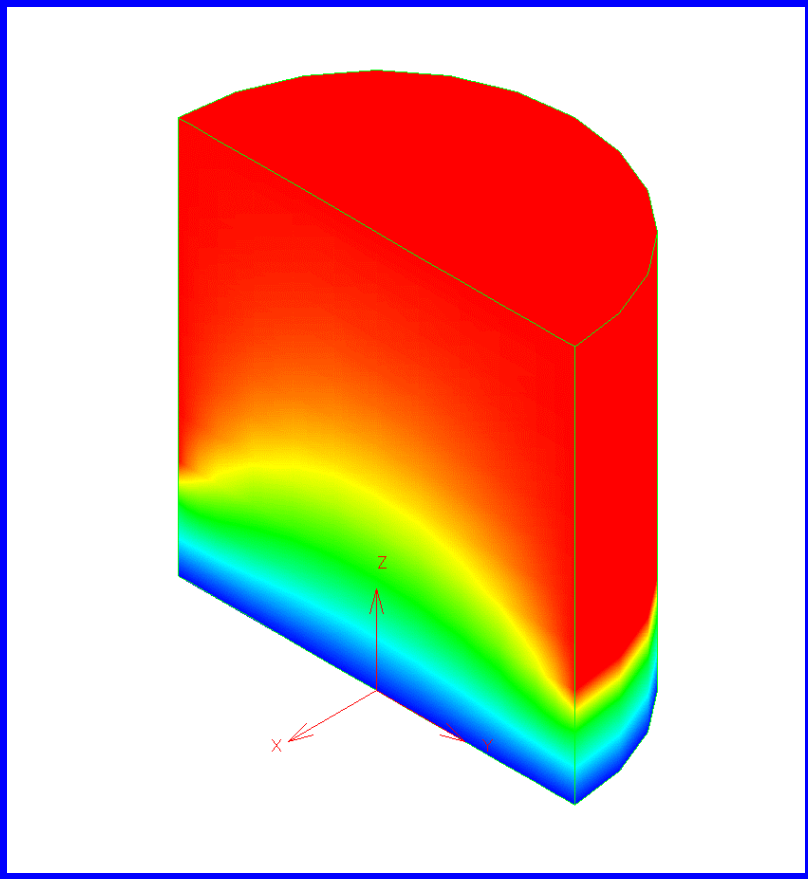

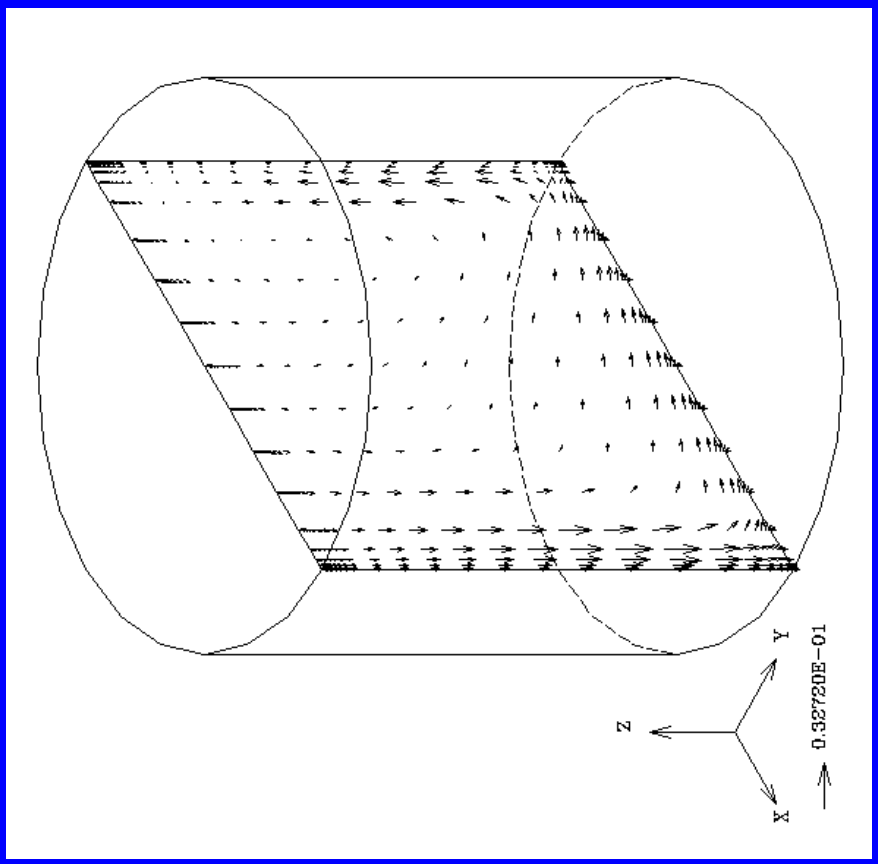
Y
Z
X
0.32720E-01

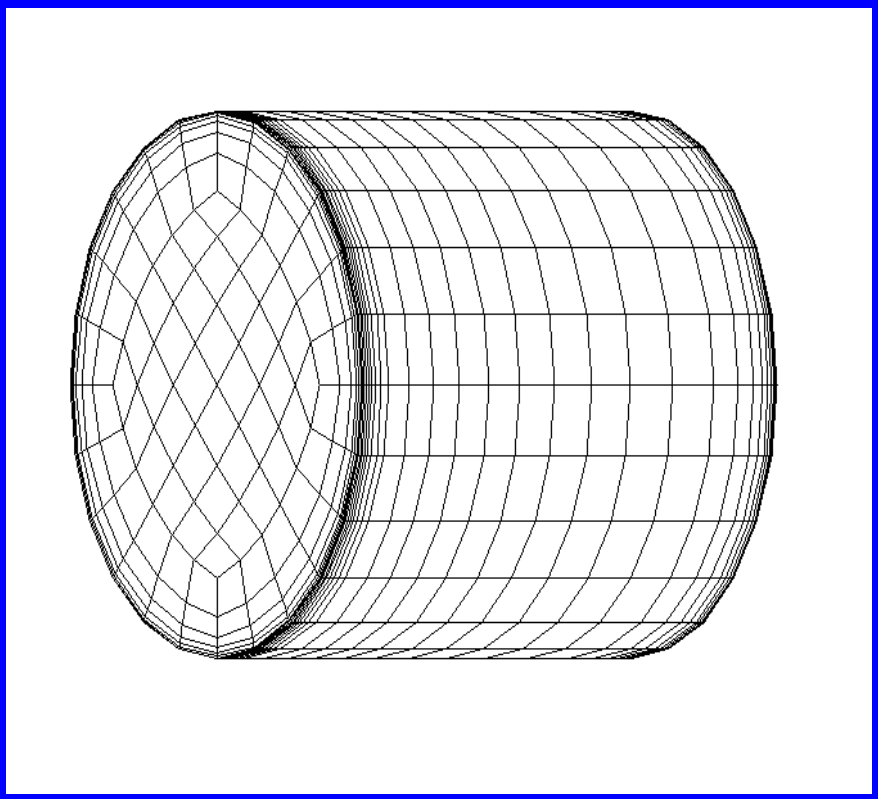

Magnetic field effects on g-jitter induced flows and mass transfer in International Space Station

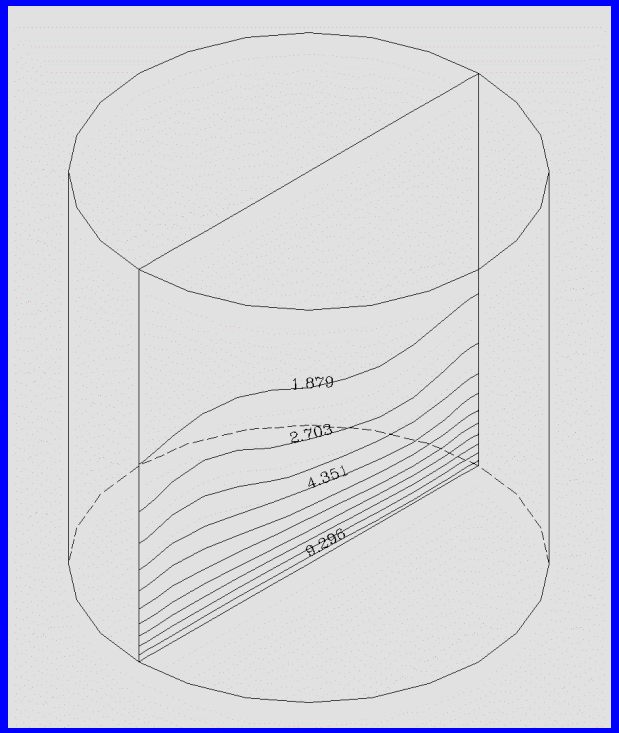

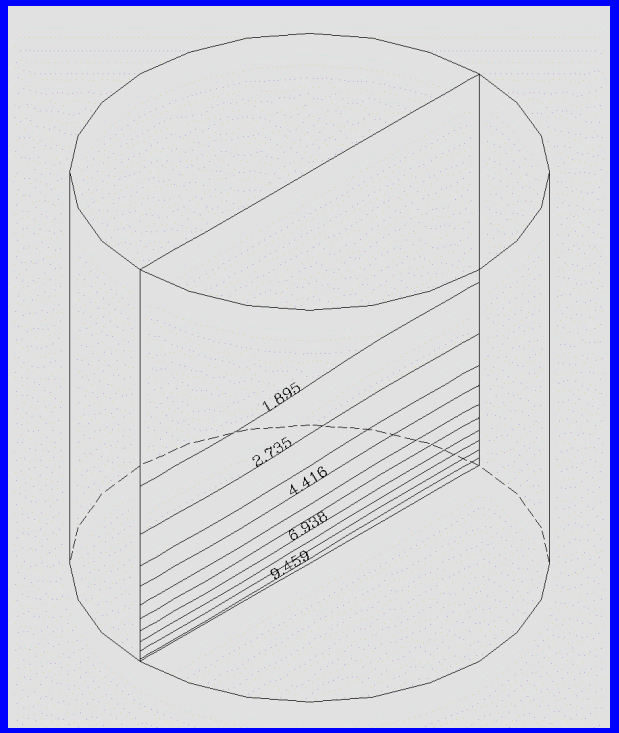

Concentration distribution without(left) and with the presence of magnetic fields in the International Space Station

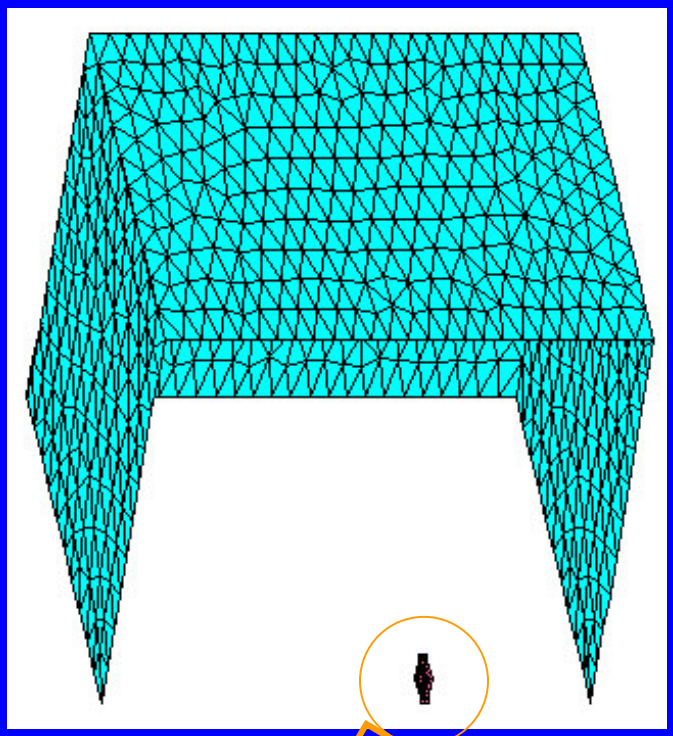

Solution strategy for nonlinear problems

- BE solution once for boundary element solution, $\mathbf{q}_I = \mathbf{M}\mathbf{A}_I + \mathbf{F}'$
- Iterative solution among the temperature and electric field in finite element solution region, that is, the foodstuff being processed in the field

Food processing

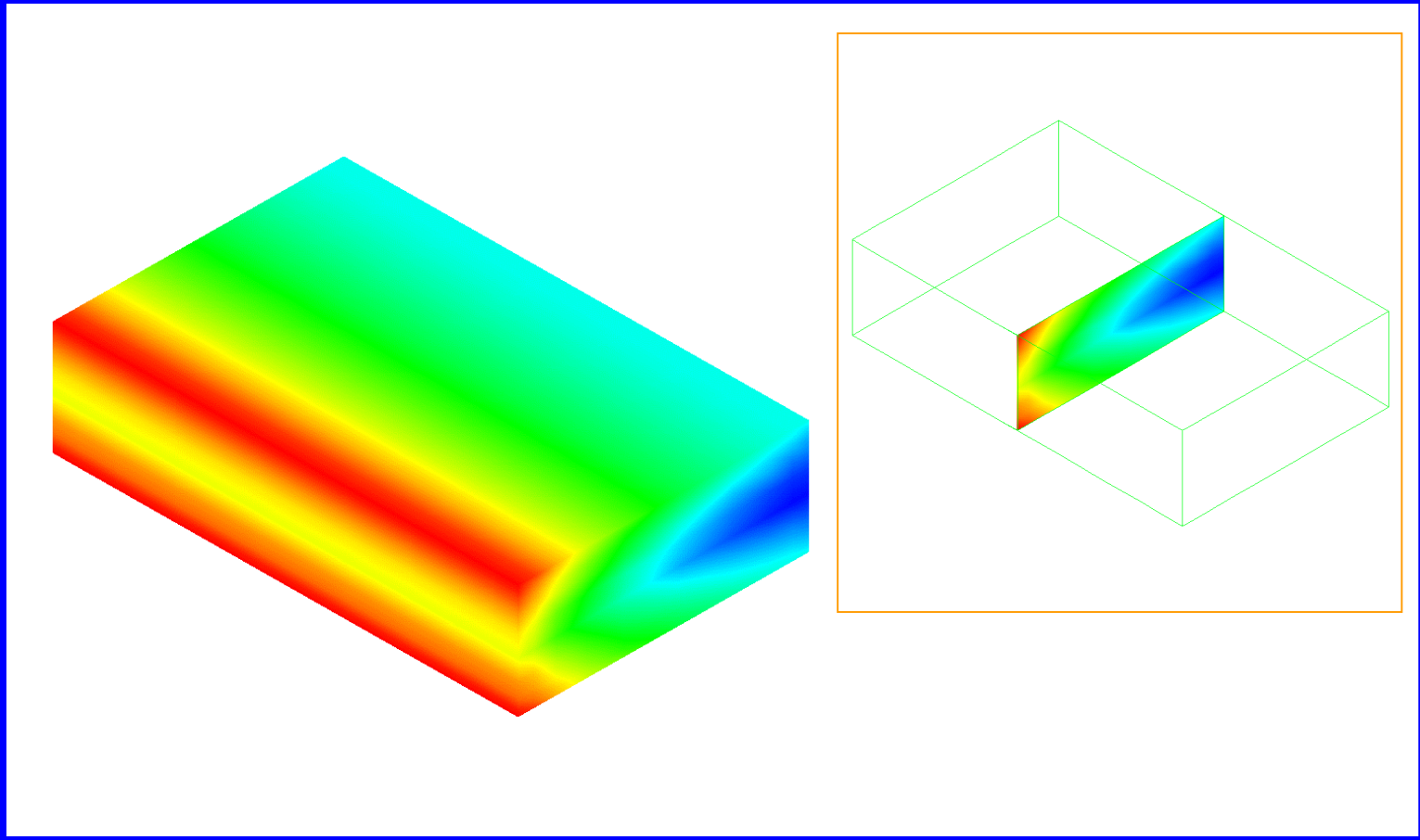

Concluding remark

We have discussed numerical simulations of coupled electromagnetic and thermal problems in processing systems resulting from inductive heating, micowave heating, and magnetohydrodynamic puming. Numerical solution methods dicussed include the finite element method, the boundary element method and the hybrid finite/boundary element method. The advantages and disadvantages of the three methods are compared. The hybrid FE/BE method appears to be better suited for coupled electromagnetic/thermal problems in processing systems. Parallel computing algorithms are also discussed, which when applied appropriately will subtantially increase computing efficiency. Minimizing the slave-master communication seems to be the key in implementing the parallel computing strategies. Examples are drawn from levitation, casting, crystal growth and food processing in microwaves. Currently, we are working on the fully 3-D FE/BE implementation and developing a numerical methodology for minimizing the temperature non-uniformity in foodstuff being processed in microwaves. The recently acquired 8-processor parallel supercomputer for our group will also help us in this endeavor.